Effective one body approach to the dynamics of two spinning black holes with next-to-leading order spin-orbit coupling

T. DAMOUR, P. JARANOWSKI and G. SCHAEFER

Institut des Hautes Études Scientifiques
35, route de Chartres
91440 – Bures-sur-Yvette (France)

Mars 2008

IHES/P/08/14

Effective one body approach to the dynamics of two spinning black holes with next-to-leading order spin-orbit coupling

Thibault Damour*
Institut des Hautes Études Scientifiques, 91440 Bures-sur-Yvette, France

Piotr Jaranowski†
Faculty of Physics, University of Białystok, Lipowa 41, 15–424 Białystok, Poland

Gerhard Schäfer‡
Theoretisch-Physikalisches Institut, Friedrich-Schiller-Universität, Max-Wien-Pl. 1, 07743 Jena, Germany

(Dated: March 7, 2008)

Using a recent, novel Hamiltonian formulation of the gravitational interaction of spinning binaries, we extend the Effective One Body (EOB) description of the dynamics of two spinning black holes to next-to-leading order (NLO) in the spin-orbit interaction. The spin-dependent EOB Hamiltonian is constructed from four main ingredients: (i) a transformation between the "effective" Hamiltonian and the "real" one, (ii) a generalized effective Hamilton-Jacobi equation involving higher powers of the momenta, (iii) a Kerr-type effective metric (with Padé-resummed coefficients) which depends on the choice of some basic "effective spin vector" $\mathbf{S}_{\rm eff}$, and which is deformed by comparable-mass effects, and (iv) an additional effective spin-orbit interaction term involving another spin vector $\boldsymbol{\sigma}$. As a first application of the new, NLO spin-dependent EOB Hamiltonian, we compute the binding energy of circular orbits (for parallel spins) as a function of the orbital frequency, and of the spin parameters. We also study the characteristics of the last stable circular orbit: binding energy, orbital frequency, and the corresponding dimensionless spin parameter $\hat{a}_{\rm LSO} \equiv cJ_{\rm LSO}/(G(H_{\rm LSO}/c^2)^2)$. We find that the inclusion of NLO spin-orbit terms has a significant "moderating" effect on the dynamical characteristics of the circular orbits for large and parallel spins.

PACS numbers: 04.25.-g, 04.25.Nx

I. INTRODUCTION

Coalescing black hole binaries are among the most promising sources for the currently operating ground-based network of interferometric detectors of gravitational waves. It is plausible that the first detections concern binary systems made of *spinning* black holes, because (as emphasized in [1]) the spin-orbit interaction can increase the binding energy of the last stable orbit, and thereby lead to larger gravitational wave emission. This makes it urgent to have template waveforms accurately describing the gravitational wave emission of spinning binary black holes. These waveforms will be functions of at least eight intrinsic real parameters: the two masses m_1, m_2 and the two spin vectors $\mathbf{S}_1$, $\mathbf{S}_2$. Due to the multi-dimensionality of the parameter space, it seems impossible for state-of-the-art numerical simulations to densely sample this parameter space. This gives a clear motivation for developing *analytical* methods for computing the needed, densely spaced, bank of accurate template waveforms.

Among existing analytical methods for computing the motion and radiation of binary black hole systems, the most complete, and the most promising one, is the Effective One Body (EOB) approach [1, 2, 3, 4]. This method was the first to provide estimates of the complete waveform (covering inspiral, plunge, merger, and ring-down) of a coalescing black hole binary, both for non-spinning systems [3], and for spinning ones [5]. Several recent works [6, 7, 8, 9, 10] have shown that there was an excellent agreement[1] between the EOB waveforms (for non-spinning systems) and the results of recent numerical simulations (see [11] for references and a review of the recent breakthroughs in numerical relativity). In addition, the EOB method predicted, before the availability of reliable numerical relativity (NR) results, a value for the final spin parameter $\hat{a}_{\rm fin}$ of a coalescing black hole binary [3, 5] which agrees within $\sim 10\%$ with the

*Electronic address: damour@ihes.fr
†Electronic address: pio@alpha.uwb.edu.pl
‡Electronic address: gos@tpi.uni-jena.de

[1] For instance, Ref. [9] finds a maximal dephasing of ± 0.005 gravitational wave cycles between EOB and numerical relativity waveforms describing 12 gravitational wave cycles corresponding to the end of the inspiral, the plunge, the merger and the beginning of the ringdown of an equal-mass coalescing binary black hole.

results of recent numerical simulations (see [11] for a review and references). Recently, it has been shown that the introduction of some refinements in the EOB approach, led to an EOB/NR agreement for $\hat{a}_{\rm fin}$ at the 2% level [12].

In a previous paper [1] the EOB method (originally developed for non-spinning systems) has been generalized to the case of spinning black holes. It was shown there that one could map the third post-Newtonian (3PN) orbital dynamics, together with the *leading order* (LO) spin-orbit and spin-spin dynamical effects of a binary system onto an *"effective test particle" moving in a Kerr-type metric*. In the present paper, we extend and refine the EOB description of spinning binaries by using a recently derived [13] *Hamiltonian* description of the spin-orbit interaction valid at the *next to leading order* (NLO) in the PN expansion. (The NLO spin-orbit effects in the harmonic-gauge equations of motion were first obtained in [14, 15].) Let us recall that LO spin-orbit effects are proportional to G/c^2, while NLO ones contain two sorts of contributions: $\propto G/c^4$ and $\propto G^2/c^4$. Regarding the spin-spin coupling terms, we shall use here only the LO results which are made of two different contributions: the LO S_1S_2 terms [16] (which have been recently extended to NLO in [17]), and the LO S_1^2 and S_2^2 terms. The latter are specific to Kerr black holes, being related to the quadrupole gravitational moment of a rotating black hole.[2] It was shown in [1] that the complete LO spin-spin terms (the sum of S_1S_2, S_1^2, and S_2^2 terms) admitted a remarkable rewriting involving a particular linear combination $\mathbf{S}_0$, defined below, of the two spin vectors. This fact, together with the more complicated structure of spin-orbit terms at the NLO, will lead us below to define a particular, improved EOB description of spinning binaries.

The present paper consists of two parts: In the first part (Sections 2 and 3) we shall develop the formalism needed to finally define (in Section 4) our improved EOB description of spinning binaries. In the second part (Section 5), we shall consider one of the simplest "applications" of our EOB Hamiltonian: a discussion of the energetics of circular, equatorial orbits for systems with parallel spins. In this section, we shall make contact with previous related analytical investigations, notably [15], and prepare the ground for making contact with numerical data.

A few words about our notation: We use the letters $a, b = 1, 2$ as particle labels. Then, m_a, $\mathbf{x}_a = (x_a^i)$, $\mathbf{p}_a = (p_{ai})$, and $\mathbf{S}_a = (S_{ai})$ denote, respectively, the mass, the position vector, the linear momentum vector, and the spin vector of the ath body; for $a \neq b$ we also define $\mathbf{r}_{ab} \equiv \mathbf{x}_a - \mathbf{x}_b$, $r_{ab} \equiv |\mathbf{r}_{ab}|$, $\mathbf{n}_{ab} \equiv \mathbf{r}_{ab}/r_{ab}$, $|\cdot|$ stands here for the Euclidean length of a 3-vector.

II. PN-EXPANDED HAMILTONIAN

Our starting point is the PN-expanded (or "Taylor-expanded") two-body Hamiltonian H which can be decomposed as the sum of: (i) an orbital part $H_{\rm o}$, (ii) a spin-orbit part $H_{\rm so}$ (linear in the spins), and (iii) a spin-spin term $H_{\rm ss}$ (quadratic in the spins),

$$H(\mathbf{x}_a, \mathbf{p}_a, \mathbf{S}_a) = H_{\rm o}(\mathbf{x}_a, \mathbf{p}_a) + H_{\rm so}(\mathbf{x}_a, \mathbf{p}_a, \mathbf{S}_a) + H_{\rm ss}(\mathbf{x}_a, \mathbf{p}_a, \mathbf{S}_a). \tag{2.1}$$

The orbital Hamiltonian $H_{\rm o}$ includes the rest-mass contribution and is explicitly known (in ADM-like coordinates) up to the 3PN order [18, 19]. Its structure is

$$H_{\rm o}(\mathbf{x}_a, \mathbf{p}_a) = \sum_a m_a c^2 + H_{\rm oN}(\mathbf{x}_a, \mathbf{p}_a) + \frac{1}{c^2} H_{\rm o1PN}(\mathbf{x}_a, \mathbf{p}_a) + \frac{1}{c^4} H_{\rm o2PN}(\mathbf{x}_a, \mathbf{p}_a) + \frac{1}{c^6} H_{\rm o3PN}(\mathbf{x}_a, \mathbf{p}_a) + \mathcal{O}\left(\frac{1}{c^8}\right). \tag{2.2}$$

The spin-orbit Hamiltonian $H_{\rm so}$ can be written as

$$H_{\rm so}(\mathbf{x}_a, \mathbf{p}_a, \mathbf{S}_a) = \sum_a \mathbf{\Omega}_a(\mathbf{x}_b, \mathbf{p}_b) \cdot \mathbf{S}_a, \tag{2.3}$$

Here, the quantity $\mathbf{\Omega}_a$ is the sum of a LO contribution ($\propto 1/c^2$) and a NLO one ($\propto 1/c^4$),

$$\mathbf{\Omega}_a(\mathbf{x}_b, \mathbf{p}_b) = \mathbf{\Omega}_a^{\rm LO}(\mathbf{x}_b, \mathbf{p}_b) + \mathbf{\Omega}_a^{\rm NLO}(\mathbf{x}_b, \mathbf{p}_b). \tag{2.4}$$

[2] Note in passing that, if one wishes to describe the dynamics of, say, neutron-star binaries with the EOB formalism, one should add "correcting" S_1^2 and S_2^2 terms.

The 3-vectors $\mathbf{\Omega}_a^{\rm LO}$ and $\mathbf{\Omega}_a^{\rm NLO}$ were explicitly computed in Ref. [13]. They are given, for the particle label $a=1$, by

$$\mathbf{\Omega}_1^{\rm LO} = \frac{G}{c^2 r_{12}^2}\left(\frac{3m_2}{2m_1}\mathbf{n}_{12}\times\mathbf{p}_1 - 2\mathbf{n}_{12}\times\mathbf{p}_2\right), \tag{2.5a}$$

$$\begin{aligned}\mathbf{\Omega}_1^{\rm NLO} = {}& \frac{G^2}{c^4 r_{12}^3}\left(\left(-\frac{11}{2}m_2 - 5\frac{m_2^2}{m_1}\right)\mathbf{n}_{12}\times\mathbf{p}_1 + \left(6m_1+\frac{15}{2}m_2\right)\mathbf{n}_{12}\times\mathbf{p}_2\right)\\ &+\frac{G}{c^4 r_{12}^2}\left(\left(-\frac{5m_2\mathbf{p}_1^2}{8m_1^3} - \frac{3(\mathbf{p}_1\cdot\mathbf{p}_2)}{4m_1^2} + \frac{3\mathbf{p}_2^2}{4m_1m_2} - \frac{3(\mathbf{n}_{12}\cdot\mathbf{p}_1)(\mathbf{n}_{12}\cdot\mathbf{p}_2)}{4m_1^2} - \frac{3(\mathbf{n}_{12}\cdot\mathbf{p}_2)^2}{2m_1m_2}\right)\mathbf{n}_{12}\times\mathbf{p}_1\right.\\ &\left.+\left(\frac{(\mathbf{p}_1\cdot\mathbf{p}_2)}{m_1m_2} + \frac{3(\mathbf{n}_{12}\cdot\mathbf{p}_1)(\mathbf{n}_{12}\cdot\mathbf{p}_2)}{m_1m_2}\right)\mathbf{n}_{12}\times\mathbf{p}_2 + \left(\frac{3(\mathbf{n}_{12}\cdot\mathbf{p}_1)}{4m_1^2} - \frac{2(\mathbf{n}_{12}\cdot\mathbf{p}_2)}{m_1m_2}\right)\mathbf{p}_1\times\mathbf{p}_2\right).\end{aligned} \tag{2.5b}$$

The expressions for $\mathbf{\Omega}_2^{\rm LO}$ and $\mathbf{\Omega}_2^{\rm NLO}$ can be obtained from the above formulas by exchanging the particle labels 1 and 2.

Let us now focus our attention on the dynamics of the *relative motion* of the two-body system in the *center-of-mass frame*, which is defined by the requirement $\mathbf{p}_1+\mathbf{p}_2=\mathbf{0}$. It will be convenient in the following to work with suitably rescaled variables. We rescale the phase-space variables $\mathbf{R}\equiv\mathbf{x}_1-\mathbf{x}_2$ and $\mathbf{P}\equiv\mathbf{p}_1=-\mathbf{p}_2$ of the relative motion as follows

$$\mathbf{r}\equiv\frac{\mathbf{R}}{GM}\equiv\frac{\mathbf{x}_1-\mathbf{x}_2}{GM},\quad \mathbf{p}\equiv\frac{\mathbf{P}}{\mu}\equiv\frac{\mathbf{p}_1}{\mu}=-\frac{\mathbf{p}_2}{\mu}, \tag{2.6}$$

where $M\equiv m_1+m_2$ and $\mu\equiv m_1m_2/M$. Note that this change of variables corresponds to rescaling the action by a factor $1/(GM\mu)$. It is also convenient to rescale the original time variable T and any part of the Hamiltonian according to

$$t\equiv\frac{T}{GM},\quad \hat{H}^{\rm NR}\equiv\frac{H^{\rm NR}}{\mu}, \tag{2.7}$$

where $H^{\rm NR}\equiv H-Mc^2$ denotes the "non relativistic" version of the Hamiltonian, i.e. the Hamiltonian without the rest-mass contribution. It has the structure $\hat{H}^{\rm NR}=\frac{1}{2}\mathbf{p}^2-\frac{1}{r}+\mathcal{O}\left(\frac{1}{c^2}\right)$.

It will be convenient in the following to work with the following two basic combinations of the spin vectors:

$$\mathbf{S}\equiv\mathbf{S}_1+\mathbf{S}_2=m_1c\,\mathbf{a}_1+m_2c\,\mathbf{a}_2, \tag{2.8a}$$

$$\mathbf{S}^*\equiv\frac{m_2}{m_1}\mathbf{S}_1+\frac{m_1}{m_2}\mathbf{S}_2=m_2c\,\mathbf{a}_1+m_1c\,\mathbf{a}_2, \tag{2.8b}$$

where we have introduced (as is usually done in the general relativistic literature) the Kerr parameters[3] of the individual black holes, $\mathbf{a}_1\equiv\mathbf{S}_1/(m_1c)$ and $\mathbf{a}_2\equiv\mathbf{S}_2/(m_2c)$. Note that, in the "spinning test mass limit" where, say, $m_2\to0$ and $S_2\to0$, while keeping $a_2=S_2/(m_2c)$ fixed, we have a "background mass" $M\simeq m_1$, a "background spin" $\mathbf{S}_{\rm bckgd}\equiv Mc\,\mathbf{a}_{\rm bckgd}\simeq\mathbf{S}_1=m_1c\,\mathbf{a}_1$, a "test mass" $\mu\simeq m_2$, and a "test spin" $\mathbf{S}_{\rm test}=\mathbf{S}_2=m_2c\,\mathbf{a}_2\simeq\mu c\,\mathbf{a}_{\rm test}$ [with $\mathbf{a}_{\rm test}\equiv\mathbf{S}_{\rm test}/(\mu c)$]. Then, in this limit the combination $\mathbf{S}\simeq\mathbf{S}_1=m_1c\,\mathbf{a}_1\simeq Mc\,\mathbf{a}_{\rm bckgd}=\mathbf{S}_{\rm bckgd}$ measures the background spin, while the other combination, $\mathbf{S}^*\simeq m_1c\,\mathbf{a}_2\simeq Mc\,\mathbf{a}_{\rm test}=M\mathbf{S}_{\rm test}/\mu$ measures the (specific) test spin $\mathbf{a}_{\rm test}=\mathbf{S}_{\rm test}/(\mu c)$. The quantities $\mathbf{S}$ and $\mathbf{S}^*$ are the two simplest *symmetric* (under the permutation $1\leftrightarrow2$) combinations of the two spin vectors which have these properties.

In view of the rescaling of the action by a factor $1/(GM\mu)$, corresponding to the rescaled phase-space variables above, it will be natural to work with correspondingly rescaled spin variables[4]

$$\bar{\mathbf{S}}^{\rm X}\equiv\frac{\mathbf{S}^{\rm X}}{GM\mu}, \tag{2.9}$$

---

[3] Note that we use here the usual definition where the Kerr parameter $a\equiv S/(Mc)$ has the dimension of length. We denote the associated dimensionless rotational parameter with an overhat: $\hat{a}\equiv a\,c^2/(GM)=cS/(GM^2)$.

[4] We recall that (orbital and spin) angular momenta have the same dimension as the action.

for any label X (X $= 1, 2, *, \cdots$).

Making use of the definitions (2.6)–(2.9) one easily gets from Eqs. (2.3)–(2.5) the center-of-mass spin-orbit Hamiltonian (divided by μ) expressed in terms of the rescaled variables:

$$\begin{aligned}\hat{H}_{\rm so}(\mathbf{r},\mathbf{p},\bar{\mathbf{S}},\bar{\mathbf{S}}^*) &= \frac{H_{\rm so}(\mathbf{r},\mathbf{p},\bar{\mathbf{S}},\bar{\mathbf{S}}^*)}{\mu}\\ &= \frac{1}{c^2}\,\hat{H}^{\rm so}_{\rm LO}(\mathbf{r},\mathbf{p},\bar{\mathbf{S}},\bar{\mathbf{S}}^*)\\ &\quad + \frac{1}{c^4}\,\hat{H}^{\rm so}_{\rm NLO}(\mathbf{r},\mathbf{p},\bar{\mathbf{S}},\bar{\mathbf{S}}^*) + \mathcal{O}\left(\frac{1}{c^6}\right),\end{aligned} \tag{2.10}$$

where (here $\mathbf{n} \equiv \mathbf{r}/|r|$)[5]

$$\hat{H}^{\rm so}_{\rm LO}(\mathbf{r},\mathbf{p},\bar{\mathbf{S}},\bar{\mathbf{S}}^*) = \frac{\nu}{r^2}\left\{2\big(\bar{S},n,p\big) + \frac{3}{2}\big(\bar{S}^*,n,p\big)\right\}, \tag{2.11a}$$

$$\begin{aligned}\hat{H}^{\rm so}_{\rm NLO}(\mathbf{r},\mathbf{p},\bar{\mathbf{S}},\bar{\mathbf{S}}^*) &= \frac{\nu}{r^3}\left\{ -(6+2\nu)\,\big(\bar{S},n,p\big) - (5+2\nu)\,\big(\bar{S}^*,n,p\big)\right\}\\ &\quad + \frac{\nu}{r^2}\left\{\left(\frac{19}{8}\nu\,\mathbf{p}^2 + \frac{3}{2}\nu\,(\mathbf{n}\cdot\mathbf{p})^2\right)\big(\bar{S},n,p\big)\right.\\ &\quad\left. + \left(\left(-\frac{5}{8}+2\nu\right)\mathbf{p}^2 + \frac{3}{4}\nu\,(\mathbf{n}\cdot\mathbf{p})^2\right)\big(\bar{S}^*,n,p\big)\right\},\end{aligned} \tag{2.11b}$$

with $\nu \equiv \mu/M$ ranging from 0 (test-body limit) to 1/4 (equal-mass case).

Note that the structure of the rescaled spin-orbit Hamiltonian is

$$\hat{H}_{\rm so}(\mathbf{r},\mathbf{p},\bar{\mathbf{S}},\bar{\mathbf{S}}^*) = \frac{\nu}{c^2 r^2}\Big(g_S^{\rm ADM}\big(\bar{S},n,p\big) + g_{S^*}^{\rm ADM}\big(\bar{S}^*,n,p\big)\Big). \tag{2.12}$$

This corresponds to an unrescaled spin-orbit Hamiltonian of the form

$$H_{\rm so} = \frac{G}{c^2}\frac{\mathbf{L}}{R^3}\cdot\Big(g_S^{\rm ADM}\mathbf{S} + g_{S^*}^{\rm ADM}\mathbf{S}^*\Big), \tag{2.13}$$

where $R = GMr$ is the unrescaled relative distance (in ADM coordinates), $\mathbf{L} \equiv \mathbf{R}\times\mathbf{P} = GM\mu\mathbf{r}\times\mathbf{p}$ the relative orbital angular momentum, and where we have introduced two dimensionless coefficients which might be called the "gyro-gravitomagnetic ratios", because they parametrize the coupling between the spin vectors and the "apparent" gravitomagnetic field

$$\mathbf{v}\times\nabla\frac{GM}{c^2 R} \propto \frac{\mathbf{R}\times\mathbf{P}}{R^3}$$

seen in the rest-frame of a moving particle (see, e.g., Refs. [20, 21] for a discussion of the expression of the "gravitomagnetic field" in the rest-frame of a moving body). The explicit expressions of these two gyro-gravitomagnetic ratios are

$$g_S^{\rm ADM} = 2 + \frac{1}{c^2}\left(\frac{19}{8}\nu\,\mathbf{p}^2 + \frac{3}{2}\nu\,(\mathbf{n}\cdot\mathbf{p})^2 - \Big(6+2\nu\Big)\frac{1}{r}\right), \tag{2.14a}$$

$$g_{S^*}^{\rm ADM} = \frac{3}{2} + \frac{1}{c^2}\left(\Big(-\frac{5}{8}+2\nu\Big)\mathbf{p}^2 + \frac{3}{4}\nu\,(\mathbf{n}\cdot\mathbf{p})^2 - \Big(5+2\nu\Big)\frac{1}{r}\right). \tag{2.14b}$$

---

[5] We introduce the following notation for the Euclidean mixed product of 3-vectors: $(V_1,V_2,V_3) \equiv \mathbf{V}_1\cdot(\mathbf{V}_2\times\mathbf{V}_3) = \varepsilon_{ijk}V_1^i V_2^j V_3^k$.

In the following we shall introduce two related "effective" "gyro-gravitomagnetic ratios", that enter the effective EOB Hamiltonian (in effective coordinates). The label "ADM" on the gyro-gravitomagnetic ratios (2.14) is a reminder of the fact that the NLO value of these ratios depend on the precise definition of the radial distance R (which is coordinate dependent). Let us, however, briefly discuss the origin of the (coordinate-independent) LO values of these ratios, namely

$$g_S^{\rm LO} = 2, \quad g_{S^*}^{\rm LO} = \frac{3}{2} = 2 - \frac{1}{2}. \tag{2.15}$$

Here the basic ratio 2 which enters both $g_S^{\rm LO}$ and $g_{S^*}^{\rm LO}$ comes from the leading interaction, predicted by the Kerr metric, between the orbital angular momentum of a test particle and the background spin. See Eq. (4.17) below. As for the $-\frac{1}{2}$ "correction" in the coupling of the "test mass" spin combination $\mathbf{S}^*$ it can be seen (e.g. from Eq. (3.6b) of [22]) to come from the famous $\frac{1}{2}$ factor in the Thomas precession (which is a universal, special relativistic effect, separate from the effects which are specific to the gravitational interaction, see Eqs. (3.2) and (3.3) in [22]).

To complete this Section, let us recall the remarkable form [found in Ref. [1], see Eq. (2.54) there] of the leading-order spin-spin Hamiltonian $H_{\rm ss}$ (including S_1^2, S_2^2 as well as $S_1 S_2$ terms). The unrescaled form of the spin-spin Hamiltonian reads

$$H_{\rm ss}(\mathbf{R}, \mathbf{S}_0) = \frac{\nu}{2} \frac{G}{c^2} S_0^i S_0^j \partial_{ij} \frac{1}{R}, \tag{2.16}$$

while its rescaled version reads

$$\begin{aligned} \hat{H}_{\rm ss}(\mathbf{r}, \bar{\mathbf{S}}_0) &\equiv \frac{H_{\rm ss}(\mathbf{R}, \mathbf{S}_0)}{\mu} \\ &= \frac{1}{2} \frac{\nu^2}{c^2} \bar{S}_0^i \bar{S}_0^j \partial_{ij} \frac{1}{r} = \frac{1}{2} \frac{\nu^2}{c^2} \frac{3(\mathbf{n} \cdot \bar{\mathbf{S}}_0)^2 - \bar{\mathbf{S}}_0^2}{r^3}. \end{aligned} \tag{2.17}$$

The remarkable fact about this result is that it is entirely expressible in terms of the specific combination of spins $\mathbf{S}_0 \equiv GM\mu \bar{\mathbf{S}}_0$ defined as:

$$\mathbf{S}_0 \equiv \mathbf{S} + \mathbf{S}^* = \Big(1 + \frac{m_2}{m_1}\Big)\mathbf{S}_1 + \Big(1 + \frac{m_1}{m_2}\Big)\mathbf{S}_2. \tag{2.18}$$

We shall come back below to the remarkable properties of the combination $\mathbf{S}_0$, which will play a central role in our EOB construction.

III. EFFECTIVE HAMILTONIAN AND "EFFECTIVE GYRO-GRAVITOMAGNETIC" RATIOS

We have obtained in the previous Section the expression of the full center-of-mass-frame Hamiltonian (2.1), in PN-expanded form. In order to transform this Hamiltonian into a format which can be resummed in a manner compatible with previous work on the EOB formalism, we need to perform two operations on the Hamiltonian (2.1). First, we need to transform the phase-space coordinates $(\mathbf{x}_a, \mathbf{p}_a, \mathbf{S}_a)$ by a canonical transformation compatible with the one used in previous EOB work. Second, we need to compute the *effective* Hamiltonian corresponding to the (canonically transformed) *real* Hamiltonian (2.1).

We start by performing the purely orbital canonical transformation which was found to be needed in Refs. [2, 4] to go from the ADM coordinates (used in the PN-expanded dynamics) to the coordinates used in the EOB dynamics. This orbital canonical transformation is (implicitly) given by

$$x'^i = x^i + \frac{\partial G_{\rm o}(x, p')}{\partial p'_i}, \quad p'_i = p_i - \frac{\partial G_{\rm o}(x, p')}{\partial x^i}. \tag{3.1}$$

Here the orbital generating function $G_{\rm o}(q, p')$ has been derived to 2PN accuracy in [2], and to 3PN accuracy in [4]. In the present paper, as we are only concerned with the additional spin-orbit terms, treated to 1PN fractional accuracy, it is enough to work with the 1PN-accurate generating function $G_{\rm o}(x, p')$. In terms of the rescaled variables, the rescaled 1PN-accurate orbital generating function reads

$$\bar{G}_{\rm o}(\mathbf{r}, \mathbf{p}) \equiv \frac{G_{\rm o}(\mathbf{r}, \mathbf{p})}{GM\mu}$$

$$= \frac{1}{c^2}(\mathbf{r}\cdot\mathbf{p})\left(-\frac{1}{2}\nu\,\mathbf{p}^2 + \Big(1+\frac{1}{2}\nu\Big)\frac{1}{r}\right). \tag{3.2}$$

This transformation changes the phase-space variables from $(\mathbf{r},\mathbf{p},\bar{\mathbf{S}},\bar{\mathbf{S}}^*)$ to $(\mathbf{r}',\mathbf{p}',\bar{\mathbf{S}},\bar{\mathbf{S}}^*)$. At the linear order in the transformation (which will be enough for our purpose), the effect of the transformation on any of the phase-space variable, say y, is $y' = y + \{y, G_{\rm o}\}$, where $\{\cdot,\cdot\}$ denotes the Poisson bracket. As $G_{\rm o}$ is independent of time, it leaves the Hamiltonian numerically invariant: $H'(y') = H(y)$. This means that it changes the *functional* form of the Hamiltonian according to $H'(y') = H(y' - \{y, G_{\rm o}\}) = H(y') - \{H, G_{\rm o}\}$. Note the appearance of the opposite sign in front of the Poisson bracket, with respect to the effect of the generating function on the phase-space variables.

As $G_{\rm o}$ is of order $1/c^2$, its explicit effect on the two separate terms, $H^{\rm so}_{\rm LO}$ and $H^{\rm so}_{\rm NLO}$, in the PN expansion of the spin-orbit Hamiltonian is given by:

$$H'^{\rm so}_{\rm LO}(\mathbf{r}',\mathbf{p}',\bar{\mathbf{S}},\bar{\mathbf{S}}^*) = H^{\rm so}_{\rm LO}(\mathbf{r}',\mathbf{p}',\bar{\mathbf{S}},\bar{\mathbf{S}}^*), \tag{3.3a}$$

$$\begin{aligned} H'^{\rm so}_{\rm NLO}(\mathbf{r}',\mathbf{p}',\bar{\mathbf{S}},\bar{\mathbf{S}}^*) &= H^{\rm so}_{\rm NLO}(\mathbf{r}',\mathbf{p}',\bar{\mathbf{S}},\bar{\mathbf{S}}^*) \\ &\quad - \{H^{\rm so}_{\rm LO}, \bar{G}_{\rm o}\}(\mathbf{r}',\mathbf{p}',\bar{\mathbf{S}},\bar{\mathbf{S}}^*). \end{aligned} \tag{3.3b}$$

It will be convenient in the following to further transform the phase-space variables by performing a secondary, purely spin-dependent canonical transformation, affecting only the NLO spin-orbit terms. The associated new generating function, $G_{\rm s}(\mathbf{r},\mathbf{p},\bar{\mathbf{S}},\bar{\mathbf{S}}^*)$ (assumed to be proportional to the spins and of order $1/c^4$) will change the variables $(y') \equiv (\mathbf{r}',\mathbf{p}',\bar{\mathbf{S}},\bar{\mathbf{S}}^*)$ into $(y'') \equiv (\mathbf{r}'',\mathbf{p}'',\bar{\mathbf{S}}'',\bar{\mathbf{S}}''^*)$ according to the general rule[6] $y'' = y' + \{y', G_{\rm s}\}$. For the same reason as above, the (first-order) effect of $G_{\rm s}$ on the functional form of the Hamiltonian will involve a Poisson bracket with the opposite sign: $H''(y'') = H(y'') - \{H, G_{\rm s}\}$.

We shall consider a generating function whose unrescaled form reads

$$G_{\rm s}(\mathbf{R},\mathbf{P},\mathbf{S},\mathbf{S}^*) = \frac{G}{\mu\,c^4}\frac{1}{R^3}(\mathbf{R}\cdot\mathbf{P})(\mathbf{R}\times\mathbf{P})\cdot\Big(a(\nu)\,\mathbf{S} + b(\nu)\,\mathbf{S}^*\Big), \tag{3.4}$$

while its rescaled form reads

$$\begin{aligned} \bar{G}_{\rm s}(\mathbf{r},\mathbf{p},\bar{\mathbf{S}},\bar{\mathbf{S}}^*) &\equiv \frac{G_{\rm s}(\mathbf{R},\mathbf{P},\mathbf{S},\mathbf{S}^*)}{GM\mu} \\ &= \frac{1}{c^4}\nu\frac{(\mathbf{n}\cdot\mathbf{p})}{r}\left(a(\nu)\big(\bar{S},n,p\big) + b(\nu)\big(\bar{S}^*,n,p\big)\right). \end{aligned} \tag{3.5}$$

Here $a(\nu)$ and $b(\nu)$ are two arbitrary, ν-dependent dimensionless coefficients.[7] Similarly to the result above, the explicit effect of this new canonical transformation on the two separate terms, $H'^{\rm so}_{\rm LO}$ and $H'^{\rm so}_{\rm NLO}$, in the PN expansion of the spin-orbit Hamiltonian reads:

$$H''^{\rm so}_{\rm LO}(\mathbf{r}'',\mathbf{p}'',\bar{\mathbf{S}}'',\bar{\mathbf{S}}''^*) = H'^{\rm so}_{\rm LO}(\mathbf{r}'',\mathbf{p}'',\bar{\mathbf{S}}'',\bar{\mathbf{S}}''^*), \tag{3.6a}$$

$$\begin{aligned} H''^{\rm so}_{\rm NLO}(\mathbf{r}'',\mathbf{p}'',\bar{\mathbf{S}}'',\bar{\mathbf{S}}''^*) &= H'^{\rm so}_{\rm NLO}(\mathbf{r}'',\mathbf{p}'',\bar{\mathbf{S}}'',\bar{\mathbf{S}}''^*) \\ &\quad - \{H_{\rm oN}, \bar{G}_{\rm s}\}(\mathbf{r}'',\mathbf{p}'',\bar{\mathbf{S}}'',\bar{\mathbf{S}}''^*), \end{aligned} \tag{3.6b}$$

where $H_{\rm oN}$ is the Newtonian orbital Hamiltonian. In the following, we shall, for simplicity of notation, omit the double primes on the new phase-space variables (and on the corresponding Hamiltonian).

The second operation we need to do is to connect the "real" Hamiltonian H to the "effective" one $H_{\rm eff}$, which is more closely linked to the description of the EOB quasi-geodesic dynamics. The relation between the two Hamiltonians is quite simple [2, 4]:

$$\frac{H_{\rm eff}}{\mu c^2} \equiv \frac{H^2 - m_1^2c^4 - m_2^2c^4}{2m_1m_2c^4}, \tag{3.7}$$

---

[6] Note that while $G_{\rm o}$ did not affect the spin variables, the spin-dependent generating function $G_{\rm s}$ will now affect them.

[7] The coefficients $a(\nu)$ and $b(\nu)$ can be thought of as being two "gauge" parameters, related to the arbitrariness in choosing a spin-supplementary condition, and in defining a local frame to measure the spin vectors.

where we recall that the real Hamiltonian H contains the rest-mass contribution $Mc^2 = (m_1 + m_2)c^2$. Let us also note that Eq. (3.7) is equivalent to

$$\frac{H_{\rm eff}}{\mu c^2} = 1 + \frac{H^{\rm NR}}{\mu c^2} + \frac{1}{2}\nu\frac{(H^{\rm NR})^2}{\mu^2 c^4}, \tag{3.8}$$

where $H^{\rm NR}$ denotes the "non relativistic" part of the total Hamiltonian H, i.e., $H^{\rm NR} \equiv H - Mc^2$, or more explicitly

$$H^{\rm NR} = \Big(H_{\rm oN} + \frac{H_{\rm o1PN}}{c^2} + \frac{H_{\rm o2PN}}{c^4} + \frac{H_{\rm o3PN}}{c^6}\Big) + \Big(\frac{H^{\rm so}_{\rm LO}}{c^2} + \frac{H^{\rm so}_{\rm NLO}}{c^4}\Big). \tag{3.9}$$

By expanding (in powers of $1/c^2$ and in powers of the spins) the exact effective Hamiltonian (3.7), one easily finds that the "spin-orbit part" of the effective Hamiltonian $H_{\rm eff}$ (i.e. the part which is linear-in-spin) differs from the corresponding part $H_{\rm so}$ in the "real" Hamiltonian by a factor $\simeq 1 + \nu\hat{H}^{\rm NR}/c^2 \simeq 1 + \nu\hat{H}_{\rm oN}/c^2$, so that we get, for the explicit PN expansion of $H^{\rm so}_{\rm eff}$,

$$\frac{H^{\rm so}_{\rm eff}}{\mu} = \frac{1}{c^2}\hat{H}^{\rm so}_{\rm LO} + \frac{1}{c^4}\Big(\hat{H}^{\rm so}_{\rm NLO} + \nu\hat{H}_{\rm oN}\hat{H}^{\rm so}_{\rm LO}\Big). \tag{3.10}$$

Combining this result with the effect of the two generating functions discussed above (and omitting, as we already said, the double primes on the new phase-space variables $(\mathbf{r}'', \mathbf{p}'', \bar{\mathbf{S}}'', \bar{\mathbf{S}}''^*)$), we get the transformed spin-orbit part of the effective Hamiltonian in the form

$$\frac{H^{\rm so}_{\rm eff}}{\mu} = \frac{\nu}{c^2 r^2}(\mathbf{n}\times\mathbf{p})\cdot\Big(g^{\rm eff}_S\bar{\mathbf{S}} + g^{\rm eff}_{S^*}\bar{\mathbf{S}}^*\Big), \tag{3.11}$$

which corresponds to the following unrescaled form (with $\mathbf{L} \equiv \mathbf{R}\times\mathbf{P}$):

$$H^{\rm so}_{\rm eff} = \frac{G}{c^2}\frac{\mathbf{L}}{R^3}\cdot\Big(g^{\rm eff}_S\mathbf{S} + g^{\rm eff}_{S^*}\mathbf{S}^*\Big). \tag{3.12}$$

Here the two "effective gyro-gravitomagnetic" ratios $g^{\rm eff}_S$ and $g^{\rm eff}_{S^*}$ differ from the "ADM" ones introduced above by three effects: (i) a factor $\simeq 1 + \nu\hat{H}^{\rm NR}/c^2 \simeq 1 + \nu\hat{H}_{\rm oN}/c^2$ due to the transformation from H to $H_{\rm eff}$, (ii) the effect of the orbital generating function $G_{\rm o}$ going from ADM to EOB coordinates, and (iii) the effect of the spin-dependent generating function $G_{\rm s}$, which involves the gauge parameters $a(\nu)$ and $b(\nu)$. Their explicit expressions are then found to read

$$g^{\rm eff}_S \equiv 2 + \frac{1}{c^2}\bigg(\Big(\frac{3}{8}\nu + a(\nu)\Big)\mathbf{p}^2 - \Big(\frac{9}{2}\nu + 3a(\nu)\Big)(\mathbf{n}\cdot\mathbf{p})^2 - \frac{1}{r}\Big(\nu + a(\nu)\Big)\bigg), \tag{3.13a}$$

$$g^{\rm eff}_{S^*} \equiv \frac{3}{2} + \frac{1}{c^2}\bigg(\Big(-\frac{5}{8} + \frac{1}{2}\nu + b(\nu)\Big)\mathbf{p}^2 - \Big(\frac{15}{4}\nu + 3b(\nu)\Big)(\mathbf{n}\cdot\mathbf{p})^2 - \frac{1}{r}\Big(\frac{1}{2} + \frac{5}{4}\nu + b(\nu)\Big)\bigg). \tag{3.13b}$$

The choice of the two "gauge" parameters $a(\nu)$ and $b(\nu)$ is arbitrary, and physical results should not depend on them.[8] This would be the case if we were dealing with the exact Hamiltonian. However, as we work only with an approximation to the exact Hamiltonian, there will remain some (weak) dependence of our results on the choice of $a(\nu)$ and $b(\nu)$. We can use this dependence to try to simplify, and/or to render more accurate, the spin-orbit effects implied by the above expressions. In particular, we shall focus in this paper on a special simplifying choice of these gauge parameters: namely, the values

$$a(\nu) = -\frac{3}{8}\nu, \quad b(\nu) = \frac{5}{8} - \frac{1}{2}\nu, \tag{3.14}$$

which suppress the dependence of the effective gyro-gravitomagnetic ratios on $\mathbf{p}^2$. With this particular choice, the explicit expressions of these ratios become

---

[8] Note in particular that the gyro-gravitomagnetic ratios do not depend on $a(\nu)$ and $b(\nu)$ when considering circular orbits, i.e. when $\mathbf{p}^2 = 1/r$ and $(\mathbf{n}\cdot\mathbf{p}) = 0$.

$$g_S^{\rm eff} \equiv 2 + \frac{1}{c^2}\biggl(-\frac{27}{8}\nu\,(\mathbf{n}\cdot\mathbf{p})^2 - \frac{5}{8}\nu\,\frac{1}{r}\biggr), \tag{3.15a}$$

$$g_{S^*}^{\rm eff} \equiv \frac{3}{2} + \frac{1}{c^2}\biggl(-\Bigl(\frac{15}{8}+\frac{9}{4}\nu\Bigr)(\mathbf{n}\cdot\mathbf{p})^2 - \Bigl(\frac{9}{8}+\frac{3}{4}\nu\Bigr)\frac{1}{r}\biggr). \tag{3.15b}$$

IV. SPIN-DEPENDENT EFFECTIVE-ONE-BODY HAMILTONIAN

Up to now we only considered PN-expanded results. In this Section, we shall generalize the approach of [1] in incorporating, in a resummed way, the spin-dependent effects within the EOB approach. Let us first recall that the approach of [1] consists in combining three different ingredients:

- a generalized Hamilton-Jacobi equation involving higher powers of the momenta (as is necessary at the 3PN accuracy [4]);
- a ν-deformed Kerr-type metric $g^{\alpha\beta}_{\rm eff}$, which depends on the choice of some basic "effective spin vector" $S^i_{\rm eff}$;
- the possible consideration of an additional spin-orbit interaction term $\Delta H_{\rm so}(\mathbf{r},\mathbf{p},\mathbf{S}_0,\boldsymbol{\sigma})$ in the effective Hamiltonian, whose aim is to complete the spin-dependent interaction incorporated in the definition of the Hamilton-Jacobi equation based on a certain choice of "effective spin vector" $S^i_{\rm eff}$.

At the LO in spin-orbit and spin-spin interactions, Ref. [1] showed that one had the choice between two possibilities:
(i) use as effective spin vector the combination $\mathbf{S}+\frac{3}{4}\mathbf{S}^*$ which correctly describes the LO spin-orbit effects, but only approximately describes the LO spin-spin effects;[9] or
(ii) use as effective spin vector the combination

$$\mathbf{S}_0 \equiv \mathbf{S}+\mathbf{S}^* = \Bigl(1+\frac{m_2}{m_1}\Bigr)\mathbf{S}_1 + \Bigl(1+\frac{m_1}{m_2}\Bigr)\mathbf{S}_2, \tag{4.1}$$

which correctly describes the full LO spin-spin interaction (see (2.17) above), and complete the description of the LO spin-orbit effects by adding a term $\Delta H_{\rm so}(\mathbf{r},\mathbf{p},\mathbf{S}_0,\boldsymbol{\sigma})$ involving a suitably defined spin combination $\boldsymbol{\sigma}$. (At LO, Ref. [1] defined $\boldsymbol{\sigma}^{\rm LO} = -\frac{1}{4}\mathbf{S}^*$.)

Intuitively speaking, the second possibility consists in considering that the "effective particle" is endowed not only with a mass μ, but also with a "spin" proportional to $\boldsymbol{\sigma}$, so that it interacts with the "effective background spacetime" both via a geodesic-type interaction (described by the generalized Hamilton-Jacobi equation), and via an additional spin-dependent interaction proportional to its spin $\propto \boldsymbol{\sigma}$.

At the present, NLO approximation, where it is crucial to accurately describe the spin-orbit interaction, as well as, by consistency, the LO spin-spin ones, we have chosen to follow the second possibility, which offers more flexibility, and which looks natural in view of the remarkably simple LO result (2.17) for the spin-spin interaction (see, however, the suggestion at the end of the concluding Section 6).

Therefore we shall successively introduce the ingredients needed to define

- the Hamilton-Jacobi equation (describing the basic "geodesic-type" part of the effective Hamiltonian);
- the effective, ν-deformed Kerr-type metric $g^{\alpha\beta}_{\rm eff}$;
- the "effective spin vector" $S^i_{\rm eff}$ entering the previous Kerr-type metric;
- the additional spin-orbit interaction $\Delta H_{\rm so}(\mathbf{r},\mathbf{p},\mathbf{S}_0,\boldsymbol{\sigma})$ involving a new, specific NLO spin combination $\boldsymbol{\sigma}$.

The modified Hamilton-Jacobi equation [4] is of the form

$$g^{\alpha\beta}_{\rm eff}\,P_\alpha P_\beta + Q_4(P_i) = -\mu^2 c^2, \tag{4.2}$$

[9] One can then correct for the missing terms by adding an explicit supplementary term in the Hamiltonian, quadratic in the spins.

where $Q_4(P_i)$ is a quartic-in-momenta term (which only depends on the space momentum components P_i). For circular orbits $Q_4(P_i)$ will be zero (see [1, 4]), so that we will not need its explicit expression in the present paper.

The role of the Hamilton-Jacobi equation above is to allow one to compute the main part (modulo the additional spin-orbit interaction added later) of the effective Hamiltonian $H_{\rm eff}^{\rm main} = E_{\rm eff} \equiv -P_0 c$ by solving (4.2) with respect to P_0. The result can be written as

$$H_{\rm eff}^{\rm main} = E_{\rm eff} = \beta^i P_i c + \alpha c \sqrt{\mu^2 c^2 + \gamma^{ij} P_i P_j + Q_4(P_i)}, \tag{4.3}$$

where we have introduced the auxiliary notation

$$\alpha \equiv (-g_{\rm eff}^{00})^{-1/2}, \quad \beta^i \equiv \frac{g_{\rm eff}^{0i}}{g_{\rm eff}^{00}}, \quad \gamma^{ij} \equiv g_{\rm eff}^{ij} - \frac{g_{\rm eff}^{0i} g_{\rm eff}^{0j}}{g_{\rm eff}^{00}}. \tag{4.4}$$

The next crucial ingredient consists in defining the (spin-dependent) effective metric entering the Hamilton-Jacobi equation, and thereby the effective Hamiltonian (4.3). We shall follow here Ref. [1] in employing an effective co-metric of the form (here $P_t \equiv c P_0$)

$$\begin{aligned} g_{\rm eff}^{\alpha\beta} P_\alpha P_\beta = \frac{1}{R^2 + a^2 \cos^2\theta} \Big(& \Delta_R(R)\, P_R^2 + P_\theta^2 \\ & + \frac{1}{\sin^2\theta} \Big(P_\phi + a \sin^2\theta \frac{P_t}{c} \Big)^2 \\ & - \frac{1}{\Delta_t(R)} \Big((R^2 + a^2) \frac{P_t}{c} + a\, P_\phi \Big)^2 \Big), \end{aligned} \tag{4.5}$$

where the functions Δ_t and Δ_R are defined as

$$\Delta_t(R) \equiv R^2 P_m^n \Big[A(R) + \frac{a^2}{R^2} \Big], \tag{4.6a}$$

$$\Delta_R(R) \equiv \Delta_t(R) D^{-1}(R), \tag{4.6b}$$

and where the Kerr-like parameter a is defined as $a \equiv S_{\rm eff}/(Mc)$, where $S_{\rm eff}$ denotes the modulus of the "effective spin vector" $S_{\rm eff}^i$ entering the definition of the Kerr-like metric above. We shall come back below to the choice of this vector $S_{\rm eff}^i$ (which is one of the ingredients in the definition of a spin-dependent EOB formalism). In Eq. (4.6a) P_m^n denotes the operation of taking the (n,m)-Padé approximant,[10] and the PN expansions of the metric coefficients A and D^{-1} equal (here $\hat{u} \equiv GM/(Rc^2)$)

$$A(\hat{u}) = 1 - 2\hat{u} + 2\nu\hat{u}^3 + \Big(\frac{94}{3} - \frac{41}{32}\pi^2 \Big) \nu \hat{u}^4, \tag{4.7a}$$

$$D^{-1}(\hat{u}) = 1 + 6\nu\hat{u}^2 + 2(26 - 3\nu)\nu\hat{u}^3. \tag{4.7b}$$

For pedagogical clarity, we have given above the expression of the effective EOB metric in a Boyer-Lindquist-type coordinate system aligned with the instantaneous direction of the (time-dependent) effective spin vector $S_{\rm eff}^i$. This expression will suffice in the present paper where we will only consider situations where the spin vectors are aligned with the orbital angular momentum, so that they are fixed in space. As emphasized in [1], when applying the EOB formalism to more general situations (non aligned spins) one must rewrite the effective co-metric components in a "fixed" Cartesian-like coordinate system. This is done by introducing

$$\begin{aligned} & n^i \equiv x^i/R, \quad s^i \equiv \frac{S_{\rm eff}^i}{S_{\rm eff}}, \quad \cos\theta \equiv n^i s^i, \\ & \rho \equiv \sqrt{R^2 + a^2 \cos^2\theta}, \end{aligned} \tag{4.8}$$

[10] Let us recall that the (n,m)-Padé approximant of a function $c_0 + c_1 u + c_2 u^2 + \cdots + c_{n+m} u^{n+m}$ is equal to $N_n(u)/D_m(u)$, where $N_n(u)$ and $D_m(u)$ are polynomials in u of degrees n and m, respectively.

and rewriting the co-metric components as

$$g^{00}_{\rm eff} = -\frac{(R^2+a^2)^2 - a^2\Delta_t(R)\sin^2\theta}{\rho^2\,\Delta_t(R)}, \tag{4.9a}$$

$$g^{0i}_{\rm eff} = -\frac{a(R^2+a^2-\Delta_t(R))}{\rho^2\,\Delta_t(R)}(\mathbf{s}\times\mathbf{R})^i, \tag{4.9b}$$

$$g^{ij}_{\rm eff} = \frac{1}{\rho^2}\Big(\Delta_R(R)n^in^j + R^2(\delta^{ij}-n^in^j)\Big) - \frac{a^2}{\rho^2\,\Delta_t(R)}(\mathbf{s}\times\mathbf{R})^i(\mathbf{s}\times\mathbf{R})^j. \tag{4.9c}$$

Making use of Eqs. (4.9) one computes

$$\alpha = \rho\sqrt{\frac{\Delta_t(R)}{(R^2+a^2)^2 - a^2\Delta_t(R)\sin^2\theta}}, \tag{4.10a}$$

$$\beta^i = \frac{a(R^2+a^2-\Delta_t(R))}{(R^2+a^2)^2 - a^2\Delta_t(R)\sin^2\theta}(\mathbf{s}\times\mathbf{R})^i, \tag{4.10b}$$

$$\gamma^{ij} = g^{ij}_{\rm eff} + \frac{\beta^i\beta^j}{\alpha^2}. \tag{4.10c}$$

Replacing the latter expressions in the general form of the effective energy (4.3) yields the most general form of the main part of the effective Hamiltonian $H^{\rm main}_{\rm eff}(\mathbf{x},\mathbf{P},\mathbf{S}_a)$.

The definition of $H^{\rm main}_{\rm eff}(\mathbf{x},\mathbf{P},\mathbf{S}_a)$ crucially depends on the choice of effective Kerr-type spin vector. In order to automatically incorporate, in a correct manner, the LO spin-spin terms, we shall use here

$$Mc\,\mathbf{a} \equiv \mathbf{S}_{\rm eff} \equiv \mathbf{S}_0 = \mathbf{S}+\mathbf{S}^* = \Big(1+\frac{m_2}{m_1}\Big)\mathbf{S}_1 + \Big(1+\frac{m_1}{m_2}\Big)\mathbf{S}_2. \tag{4.11}$$

Note that, besides its usefulness in treating spin-spin effects, this definition has several nice features. For example, if we introduce the Kerr parameters of the individual black holes, $\mathbf{a}_1 \equiv \mathbf{S}_1/(Mc)$, $\mathbf{a}_2 \equiv \mathbf{S}_2/(Mc)$, the Kerr parameter $\mathbf{a}_0 \equiv \mathbf{S}_0/(Mc)$ (where we naturally take $m_0 = M = m_1+m_2$) associated to the spin combination (4.1) is simply

$$\mathbf{a}_0 = \mathbf{a}_1 + \mathbf{a}_2. \tag{4.12}$$

Let us also note that the corresponding *dimensionless* spin parameters (with, again, $m_0 = M = m_1+m_2$)

$$\hat{\mathbf{a}}_i \equiv \frac{c\,\mathbf{S}_i}{Gm_i^2}, \quad i=0,1,2, \tag{4.13}$$

satisfy

$$\hat{\mathbf{a}}_0 = X_1\hat{\mathbf{a}}_1 + X_2\hat{\mathbf{a}}_2, \tag{4.14}$$

where $X_1 \equiv m_1/M$ and $X_2 \equiv m_2/M$ are the two dimensionless mass ratios (with $X_1+X_2=1$ and $X_1X_2=\nu$). This last result shows that, in $\hat{\mathbf{a}}$-space, the "point" $\hat{\mathbf{a}}_0$ is on the straight-line segment joining the two "points" $\hat{\mathbf{a}}_1$ and $\hat{\mathbf{a}}_2$. The individual Kerr bounds tell us that each point $\hat{\mathbf{a}}_1$ and $\hat{\mathbf{a}}_2$ is contained within the unit Euclidean sphere. By convexity of the unit ball, we conclude that the "effective" dimensionles spin parameter $\hat{\mathbf{a}}_0$ will also automatically satisfy the Kerr bound $|\hat{\mathbf{a}}_0| \leq 1$. This is a nice consistency feature of the definition of the associated Kerr-type metric.

It remains to define the additional "test-spin" vector $\boldsymbol{\sigma}$, and the associated additional effective spin-orbit interaction term. Following the logic of [1] (and generalizing the LO results given in Eqs. (2.56)–(2.58) there), these quantities are defined by

$$\boldsymbol{\sigma} \equiv \frac{1}{2}g_S^{\rm eff}\mathbf{S} + \frac{1}{2}g_{S^*}^{\rm eff}\mathbf{S}^* - \mathbf{S}_{\rm eff} = \frac{1}{2}(g_S^{\rm eff}-2)\mathbf{S} + \frac{1}{2}(g_{S^*}^{\rm eff}-2)\mathbf{S}^*, \tag{4.15}$$

and

$$\Delta H_{\rm so}(\mathbf{x},\mathbf{P},\mathbf{S}_0,\boldsymbol{\sigma}) \equiv \frac{R^2+a_0^2-\Delta_t(R)}{(R^2+a_0^2)^2-a_0^2\Delta_t(R)\sin^2\theta_0}\frac{(P,\sigma,R)}{M}, \tag{4.16}$$

where $\mathbf{a}_0 \equiv \mathbf{S}_0/(Mc)$ and $\cos\theta_0 \equiv n^i S_0^i/|\mathbf{S}_0|$. The justification for these definitions is that the "main" Hamilton-Jacobi part of the effective Hamiltonian contains, as spin-orbit (i.e. linear-in-spin) part, the following term

$$\begin{aligned} H_{\rm so}^{\rm main\,eff} &= cP_i\big(\beta^i\big)_{\rm linear\text{-}in\text{-}spin} \\ &= cP_i\left(\frac{R^2+a_0^2-\Delta_t(R)}{(R^2+a_0^2)^2-a_0^2\Delta_t(R)\sin^2\theta_0}(\mathbf{a}_0\times\mathbf{R})^i\right)_{\rm linear\text{-}in\text{-}spin} \\ &= \frac{2GM}{cR^3}P_i(\mathbf{a}_0\times\mathbf{R})^i + (\text{NNLO corrections}) \\ &= 2\frac{G}{c^2}\frac{\mathbf{L}}{R^3}\cdot\mathbf{S}_0 + (\text{NNLO corrections}), \end{aligned} \tag{4.17}$$

where the factor $2GM$ comes from the second term in the PN expansion of $\Delta_t(R) = R^2 - 2GMR/c^2 + 2\nu(GM)^3/(R\,c^6) + (\text{quadratic-in-spin terms})$. Note that the absence of c^{-4} correction in the effective metric function $A(R)$ means that the leading term $\propto 2GM$ in the spin-orbit part of $H^{\rm main}$ is valid *both* to LO and to NLO, i.e., up to "next to next to leading order" (NNLO).

When comparing this result to the NLO result (3.12), we see that the "main" part of the effective Hamiltonian contains a spin-orbit piece which is equivalent to having effective gyro-gravitomagnetic ratios equal to $g_S^{\rm main\,eff}=2$ and $g_{S^*}^{\rm main\,eff}=2$, instead of the correct values derived above. One then easily checks that the definition above of $\boldsymbol{\sigma}$ and of the associated supplementary spin-orbit interaction $\Delta H_{\rm so}(\mathbf{x},\mathbf{P},\mathbf{S}_0,\boldsymbol{\sigma})$ has the effect of including the full result for the NLO spin-orbit interaction. It is also to be noted that the additional spin-orbit interaction $\Delta H_{\rm so}$ goes to zero proportionally to ν in the test mass limit $m_2 \to 0$ because, on the one hand, $g_S^{\rm eff}-2$ is proportional to ν (if $a(\nu)$ is), and, on the other hand, though $g_{S^*}^{\rm eff}-2$ *does not* tend to zero with ν, the second spin combination $\mathbf{S}^*$ *does* tend to zero proportionally to ν [see Eqs. (5.2) below].

Summarizing: we propose to define a total effective spin-dependent Hamiltonian of the form

$$H_{\rm eff}(\mathbf{x},\mathbf{P},\mathbf{S}_1,\mathbf{S}_2) \equiv H_{\rm eff}^{\rm main}(\mathbf{x},\mathbf{P},\mathbf{S}_0) + \Delta H_{\rm so}(\mathbf{x},\mathbf{P},\mathbf{S}_0,\boldsymbol{\sigma}), \tag{4.18}$$

where $H_{\rm eff}^{\rm main}(\mathbf{x},\mathbf{P},\mathbf{S}_0)$ is given by the right-hand side of Eq. (4.3) computed for the effective spin variable equal to $\mathbf{S}_0$ [defined in Eq. (4.1)] and where $\Delta H_{\rm so}(\mathbf{x},\mathbf{P},\mathbf{S}_0,\boldsymbol{\sigma})$ is the additional spin-orbit interaction term defined above [with $\mathbf{a}_0 \equiv \mathbf{S}_0/(Mc)$].

Finally, the *real EOB-improved* Hamiltonian (by contrast to the "effective" one) is defined by solving Eq. (3.7) with respect to $H_{\rm real} = H^{\rm NR} + Mc^2$:

$$H_{\rm real} = Mc^2\sqrt{1+2\nu\Big(\frac{H_{\rm eff}}{\mu c^2}-1\Big)}, \tag{4.19}$$

where $H_{\rm eff}$ is given in Eq. (4.18).

V. DYNAMICS OF CIRCULAR ORBITS

In this Section we shall apply the construction of the NLO spin-dependent EOB Hamiltonian to the study of the dynamics of circular orbits of binary black hole systems.

Besides the dimensionless spin parameters $\hat{\mathbf{a}}_1$ and $\hat{\mathbf{a}}_2$ already introduced above, it is convenient to introduce the dimensionless spin variables corresponding to the basic spin combinations $\mathbf{S}$ and $\mathbf{S}^*$, namely

$$\hat{\mathbf{a}} \equiv \frac{c\,\mathbf{S}}{GM^2}, \quad \hat{\mathbf{a}}^* \equiv \frac{c\,\mathbf{S}^*}{GM^2}. \tag{5.1}$$

Let us note in passing the various links between the dimensionless spin parameters that one can define [including $\hat{\mathbf{a}}_0 \equiv c\,\mathbf{S}_0/(GM^2)$ already introduced above],

$$\hat{\mathbf{a}} = X_1^2\hat{\mathbf{a}}_1 + X_2^2\hat{\mathbf{a}}_2, \quad \hat{\mathbf{a}}^* = \nu\hat{\mathbf{a}}_1 + \nu\hat{\mathbf{a}}_2, \tag{5.2a}$$

$$\hat{\mathbf{a}}_0 = \hat{\mathbf{a}} + \hat{\mathbf{a}}^* = X_1 \hat{\mathbf{a}}_1 + X_2 \hat{\mathbf{a}}_2. \tag{5.2b}$$

Here as above we use the mass ratios $X_1 \equiv m_1/M$, $X_2 \equiv m_2/M$ such that $X_1 + X_2 = 1$ and $X_1 X_2 = \nu$. Let us note that for equal-mass binaries ($m_1 = m_2$, $X_1 = X_2 = \frac{1}{2}$), with arbitrary (possibly unequal) spins, one has $\hat{\mathbf{a}} = \hat{\mathbf{a}}^* = \frac{1}{4}(\hat{\mathbf{a}}_1 + \hat{\mathbf{a}}_2) = \frac{1}{2}\hat{\mathbf{a}}_0$. Note also that, in the test-mass limit, say $m_1 \gg m_2$ so that $X_1 \to 1$ and $X_2 \to 0$, one has

$$\hat{\mathbf{a}} = \hat{\mathbf{a}}_0 = \hat{\mathbf{a}}_1, \quad \hat{\mathbf{a}}^* = 0. \tag{5.3}$$

In the general case where the spin vectors are not aligned with the (rescaled) orbital angular momentum vector[11] $\boldsymbol{\ell}$,

$$\boldsymbol{\ell} = r\, \mathbf{n} \times \mathbf{p}, \tag{5.4}$$

there exist no circular orbits. However, there exist (at least to a good approximation) some "spherical orbits", i.e. orbits that keep a constant value of the modulus of the radius vector $\mathbf{r}$, though they do not stay within one fixed plane. As discussed in [1] one can analytically study these spherical orbits within the EOB approach, and discuss, in particular, the characteristics of the *last stable spherical orbit*.

For simplicity, we shall restrict ourselves here to the situation where both individual spins are parallel (or antiparallel) to the orbital angular momentum vector $\boldsymbol{\ell}$. In that case, we can consistently set everywhere the radial momentum to zero, $p_r = \mathbf{n} \cdot \mathbf{p} = 0$, and express the (real) EOB Hamiltonian as a function of r, $\ell = p_\varphi$ (using $\mathbf{p}^2 = \ell^2/r^2$, where $\ell \equiv |\boldsymbol{\ell}|$), and of the two scalars $\hat{a}, \hat{a}^*$ measuring the projections of our basic spin combinations on the direction of the orbital angular momentum $\boldsymbol{\ell}$. They are such that

$$\hat{\mathbf{a}} \cdot \boldsymbol{\ell} = \hat{a}\, \ell, \quad \hat{\mathbf{a}}^* \cdot \boldsymbol{\ell} = \hat{a}^*\, \ell. \tag{5.5}$$

The scalars $\hat{a}$ and $\hat{a}^*$ can be either positive or negative, depending on whether, say, $\hat{\mathbf{a}}$ is parallel or antiparallel to $\boldsymbol{\ell}$.

The sequence of circular (equatorial) orbits is then determined by the constraint

$$\frac{\partial H_{\rm real}(r, \ell, \hat{a}, \hat{a}^*)}{\partial r} = 0. \tag{5.6}$$

Then, the angular velocity along each circular orbit is given by

$$\Omega \equiv \frac{1}{GM\mu} \frac{\partial H_{\rm real}(r, \ell, \hat{a}, \hat{a}^*)}{\partial \ell}. \tag{5.7}$$

As mentioned above, we have chosen the special values $a(\nu) = -\frac{3}{8}\nu$, $b(\nu) = \frac{5}{8} - \frac{1}{2}\nu$ of the two gauge parameters, to simplify the expression of the Hamiltonian.

In Figs. 1–4 we explore several aspects of the dynamics of circular orbits, using as basic diagnostic the relation between the energy and the angular velocity along the sequence of circular orbits ("binding energy curve"). More precisely, we plot the dimensionless "non relativistic" energy

$$e \equiv \frac{H_{\rm real}}{Mc^2} - 1, \tag{5.8}$$

as a function of the dimensionless angular velocity:

$$\hat{\Omega} \equiv \frac{GM}{c^3}\Omega. \tag{5.9}$$

For simplicity, we shall restrict most of our studies to *symmetric* binary systems, i.e. systems with $m_1 = m_2$ and $a_1 = a_2$. For such systems the dimensionless effective spin parameter is $\hat{a}_0 = \hat{a}_1 = \hat{a}_2$. The information contained in these figures deals with the following aspects of the description of the dynamics:

- As a warm up, and a reminder, Fig. 1 considers the case of *non-spinning binaries* (i.e. $\hat{a}_0 = 0$). This figure contrasts the behaviour of the successive PN versions of the EOB dynamics, with that of the successive PN versions of the non-resummed, "Taylor-expanded" Hamiltonian. The numbers 1,2,3 refer to 1PN, 2PN, and

[11] In the following, we switch again to the use of scaled variables: $\mathbf{r} \equiv \mathbf{R}/(GM)$, $\boldsymbol{\ell} \equiv \mathbf{L}/(GM\mu)$, and $\mathbf{p} \equiv \mathbf{P}/\mu$.

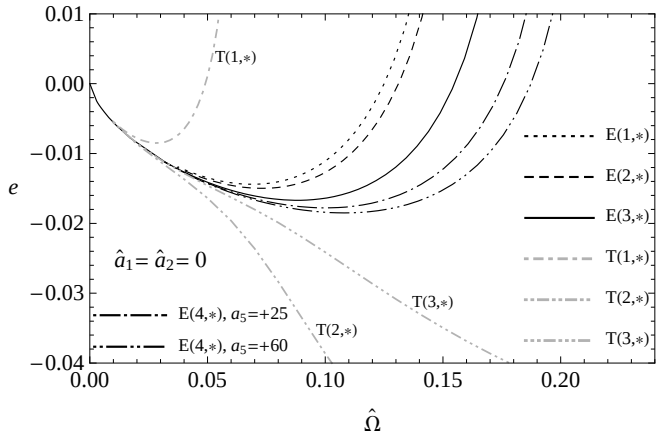

FIG. 1: Binding energy curves for circular orbits of symmetric *non-spinning* binaries ($m_1 = m_2$ and $\hat{\mathbf{a}}_1 = \hat{\mathbf{a}}_2 = \mathbf{0}$): dimensionless "non relativistic" energy e versus dimensionless angular frequency $\hat{\Omega}$. The notation E$(n, *)$ means computation of the energy using the EOB-improved real Hamiltonian (4.19) with the nPN-accurate metric function $\Delta_t(R)$; the function $\Delta_t(R)$ was computed by means of Eq. (4.6a) using the $(1, n)$ Padé approximant at the nPN order. Here $n = 1, 2, 3, 4$, where $n = 4$ refers to the "4PN" case where a term $+a_5\nu\hat{u}^5$ is added to the function $A(\hat{u})$. For the curves labelled by T$(n, *)$ the computation was done with the direct PN-expanded (ADM-coordinates) orbital Hamiltonian (2.2) with the terms up to the nPN order included.

3PN, while the letter "E" refers to "EOB" and the letter "T" refers to "Taylor". For instance, E$(3, *)$ refers to the $e(\hat{\Omega})$ binding energy curve computed with the 3PN-accurate EOB Hamiltonian. [The star in E$(3, *)$ replaces the label we shall use below to distinguish LO versus NLO treatment of spin-orbit effects. In the present non-spinning case we are insensitive to this distinction.] To be precise, the notation E$(n, *)$ refers to a computation of the circular orbits using the $\hat{a}_0 \to 0$ limit[12] of the EOB-improved real Hamiltonian (4.19) with the nPN-accurate metric function $\Delta_t(R)$; where $\Delta_t(R)$ was computed by means of Eq. (4.6b) using the following Padé approximants: (1,1) at the 1PN order, (1,2) at the 2PN order, and (1,3) at the 3PN order. As for the Taylor-based approximants to the binding energy curve, T$(n, *)$, they were computed by using as basic Hamiltonian (to define the dynamics) the nPN-accurate Taylor-expanded Hamiltonian, in ADM coordinates, (2.2), without doing any later PN re-expansion.[13]

It is interesting to note that the successive PN-approximated EOB binding energy curves are stacked in a *monotonically decreasing* fashion, when increasing the PN accuracy, and all admit a minimum at some value of the orbital frequency. This minimum corresponds to the last stable circular orbit (see below). The monotonic stacking of the EOB energy curves therefore implies that a higher PN accuracy predicts circular orbits which are more bound, and can reach higher orbital frequencies. Let us note in this respect that recent comparisons between EOB and numerical relativity data have found the need to add a *positive* 4PN additional term $+a_5\nu\hat{u}^5$ in the basic EOB radial potential $A(\hat{u})$ of Eq. (4.7a) above, with a_5 somewhere between +10 and +80 [7, 8, 9, 10]. Though we do not know yet what is the "real" value of the 4PN coefficient a_5 we have included in Fig. 1 two illustrative[14] values of this "4PN" orbital parameter, namely $a_5 = +25$ and $a_5 = +60$. Note that the effect of such positive values of a_5 is to push the last few circular orbits towards more bound, higher orbital frequency orbits. This effect will compound itself with the effects of spin explored below, and should be kept in mind when looking at our other plots.

By contrast with the "tame" and monotonic behaviour of successive EOB approximants, we see on Fig. 1 that

[12] Note that the $\hat{a}_0 \to 0$ limit of the Padé resummation of some $\hat{a}_0$-dependent metric coefficient is not necessarily the same as the Padé approximant one might normally consider in the non-spinning case.

[13] As is well-known there are always many non-equivalent ways of defining any "nPN" result, depending of where, and how, in the calculation one is replacing a function by a PN-expanded polynomial. For instance, one could PN re-expand the function giving the energy e in terms of the orbital frequency $\hat{\Omega}$, or the function giving e in terms of the orbital angular momentum L (see Ref. [4] for the computation of several such functions in the non-spinning case). However, we are ultimately interested (for gravitational-wave purposes) in defining a complete dynamics for coalescing spinning binaries. Therefore, we focus here on the results predicted by Hamiltonian functions $H(x, p, \cdots)$.

[14] These two values of the 4PN parameter a_5 were found in Refs. [7, 9] to be representative of the values of a_5 that improve the agreement between EOB waveforms and numerical relativity ones.

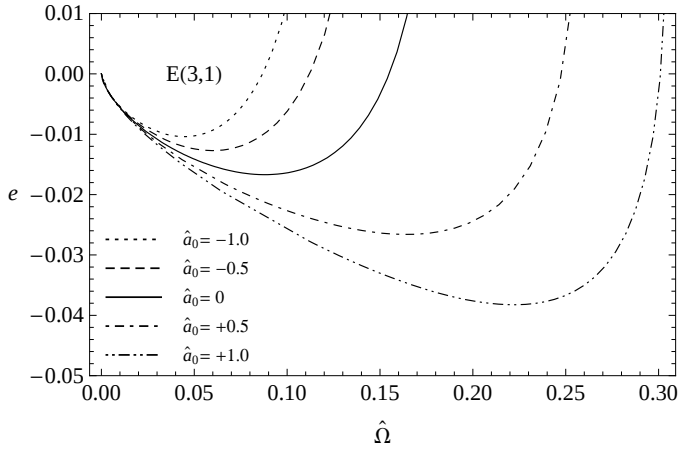

FIG. 2: Binding energy curves for circular orbits of symmetric *parallely spinning* binaries ($m_1 = m_2$ and $\hat{\mathbf{a}}_1 = \hat{\mathbf{a}}_2 \propto \mathbf{r} \times \mathbf{p}$): dimensionless energy e versus dimensionless angular frequency $\hat{\Omega}$ along circular orbits for various values of the dimensionless effective spin parameter $\hat{a}_0 \equiv c\,\mathbf{S}_0/(GM^2) = \hat{a}_1 = \hat{a}_2$ within the effective-one-body approach. The label E(3, 1) means that we use the EOB Hamiltonian with 3PN-accurate orbital effects and NLO spin-orbit coupling, i.e. Eq. (4.15) was used with the NLO gyro-gravitomagnetic ratios $g_S^{\rm eff}$ and $g_{S^*}^{\rm eff}$, Eqs. (3.13).

the successive Taylor-Hamiltonian approximants T$(n, *)$ have a more erratic behaviour. Note in particular, that the 3PN-accurate energy curve does not admit any minimum as the orbital frequency increases (in other words, there is no "last" stable circular orbit). In view of this bad behaviour of the 3PN-accurate orbital Taylor-Hamiltonian, we shall not consider anymore in the following figures the predictions coming from such Taylor Hamiltonians.[15]

- In Fig. 2 we study the effect of changing the amount of spin on the black holes of our binary system. We use here our new, NLO spin-orbit EOB Hamiltonian, as indicated by the notation E(3, 1), where the first label, 3, refers to the 3PN accuracy, and the second label, 1, to the 1PN fractional accuracy of the spin-orbit terms (i.e., the NLO accuracy). Note that the EOB binding energy curves are stacked in a monotonically decreasing way as the dimensionless effective spin $\hat{a}_0$ increases from $\hat{a}_0 = -1$ (maximal spins antiparallel to the orbital angular momentum) to $\hat{a}_0 = +1$ (maximal spins parallel to the orbital angular momentum). Note also that this curve confirms the finding of [1] that parallel spins lead to the possibility of closer and more bound circular orbits.

- Fig. 3 contrasts the effect of using the NLO spin-orbit interaction instead of the LO one in the EOB Hamiltonian. We use the full 3PN accuracy, and include the LO spin-spin interaction. E(3, 0) denotes a result obtained with the 3PN-accurate EOB Hamiltonian using the LO (or 0PN-accurate) spin-orbit terms, while E(3, 1) uses the 3PN-accurate EOB Hamiltonian with NLO (1PN-accurate) spin-orbit terms. Each panel in the Figure corresponds to a specific value of the dimensionless effective spin $\hat{a}_0$. To guide the eye we use in all our figures a solid line to denote our "best" description, i.e. the 3PN-NLO EOB E(3, 1). Note that the addition of the NLO effects in the spin-orbit interaction has the clear effect of *moderating* the influence of the spins (especially for positive spins). While the binding energy curves using the LO spin-orbit effects tend to abruptly dive down towards very negative energies when the spins are large and positive,[16] the corresponding NLO curves have a much more moderate behaviour.

Among the binding energy curves shown above, all the EOB ones (at least when the effective spin is not too large and positive), and some of the Taylor ones, admit a minimum for a certain value of the orbital frequency $\hat{\Omega}$. This minimum corresponds to an inflection point in the corresponding (EOB or Taylor) Hamiltonian considered as a

[15] Indeed, in the physically most important case of parallel (rather than anti-parallel) spins, the spin-orbit coupling will be repulsive (like the effect of a positive a_5), and will tend to reinforce the "bad" behaviour of the 3PN orbital Taylor Hamiltonian (i.e. the absence of any last stable orbit).

[16] As discussed in Section 3C of Ref. [1], this is due to the then *repulsive* character of the spin-orbit (and spin-spin) interaction.

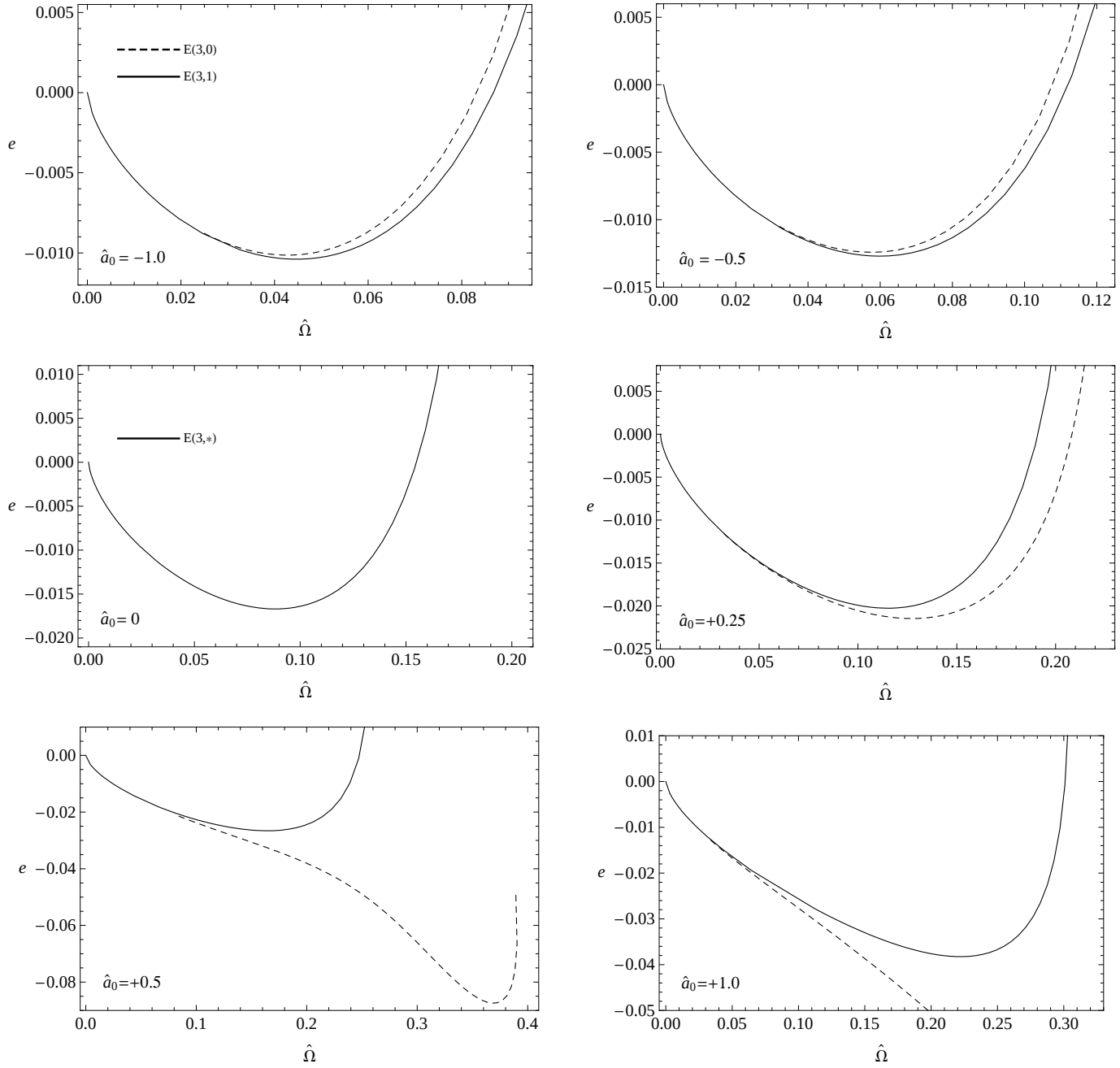

FIG. 3: Energy e versus angular frequency $\hat{\Omega}$ along circular orbits for various values of the parameter $\hat{a}_0$, as predicted by the EOB Hamiltonian. We have assumed $m_1 = m_2$, $a_1 = a_2$, and $\theta_0 = \pi/2$. As before E(n, s) refers to an EOB Hamiltonian, with nPN accuracy in the orbital terms, and an accuracy in the spin-orbit coupling equal to the LO one if $s = 0$, and the NLO one if $s = 1$. In all cases, we include the full LO spin-spin coupling.

function of r. In other words, the minimum is the solution of the two equations[17]

$$\frac{\partial H_{\rm real}}{\partial r} = 0, \quad \frac{\partial^2 H_{\rm real}}{\partial r^2} = 0. \tag{5.10}$$

[17] Note in passing that, in the EOB case, the two Eqs. (5.10) are equivalent to the two similar equations involving the *effective* Hamiltonian: $\partial H_{\rm eff}/\partial r = 0$, $\partial^2 H_{\rm eff}/\partial r^2 = 0$.

TABLE I: LSO parameters for *symmetric* binary systems (with $m_1 = m_2$ and $\hat{a}_1 = \hat{a}_2 = \hat{a}_0$) for the 3PN-NLO EOB Hamiltonian E(3, 1).

$\hat{a}_0$	e	$\hat{\Omega}$
−1.00	−0.01039	0.04473
−0.75	−0.01143	0.05139
−0.50	−0.01270	0.05989
−0.25	−0.01437	0.07143
0.00	−0.01670	0.08822
0.25	−0.02026	0.11521
0.50	−0.02660	0.16444
0.75	−0.03701	0.23249
1.00	−0.03826	0.22210

The solutions of these two simultaneous equations correspond to what we shall call here the Last Stable (circular) Orbit (LSO).[18] Several methods have been considered in the literature [4, 23] for using PN-expanded results to estimate the characteristics of the LSO. One of these methods consists in considering the minima *in the Taylor expansion of the function* $e(\hat{\Omega})$. These minima (called "Innermost Circular Orbit" (ICO) in Refs. [15, 23], where they were used to estimate the LSO of spinning binaries) differ from the minima in the Taylor energy curves considered in Fig. 1 above, which were based on using a Taylor-expanded Hamiltonian. The advantage of consistently working (as we do here) within a Hamiltonian formalism is that we are guaranteed that the minima in the corresponding energy curves, when they exist, do correspond to a Last Stable orbit (and an associated inflection point) for some well-defined underlying dynamics. By contrast the dynamical meaning (if any) of a minimum of the Taylor-expanded function $e^{\rm Taylor}(\hat{\Omega})$ is unclear. Anyway, as we saw above that the 3PN-accurate Taylor-expanded orbital Hamiltonian does not admit any Last Stable Orbit, we have not plotted in Fig. 4 the Taylor-based predictions for spinning binaries because they do not seem to lead to reasonable results.

Concerning the dynamical meaning of the LSO, let us recall that it had been analytically predicted in [3] (and confirmed in recent numerical simulations [11]) that the transition between inspiral and plunge is smooth and progressive, so that the passage through the LSO is *blurred*. In spite of the inherent "fuzziness" in the definition of the LSO, it is still interesting to delineate its dynamical characteristics because they strongly influence some of the gross features of the GW signal emitted by coalescing binaries (such as the total emitted energy, and the frequency of maximal emission).

Let us comment on the results of our study of the characteristics of LSO's:

- In Fig. 4 we plot the LSO binding energy, predicted by the EOB approach, as a function of the dimensionless effective spin parameter $\hat{a}_0$. We contrast LO spin-orbit versus NLO spin-orbit (1 versus 0). We use 3PN accuracy (for the orbital effects) in all cases, and always include the LO spin-spin interaction. The upper panel shows that the use of LO spin-orbit interactions leads to dramatically negative LSO binding energies when the spins become moderately large. [The middle panel is a close-up of the upper one, and focuses on spins $\hat{a}_0 \leq +0.2$.] We find that the 3PN-LO EOB Hamiltonian E(3, 0) admits an LSO only up to spins as large as: $\hat{a}_0 \leq +0.9$. However, as first found in [1], spin effects become dramatically (and suspiciously) large already when $\hat{a}_0 \geq +0.5$. By contrast, as we found above, the inclusion of NLO spin-orbit interactions has the effect of *moderating* the dynamical influence of high (positive) spins. The bottom panel focusses on our "best bet" 3PN-NLO Hamiltonian E(3, 1).

  As mentioned above, Ref. [15] has considered, instead of the Taylor-Hamiltonian LSO, the minimum of the Taylor-expanded function $e^{\rm Taylor}(\hat{\Omega})$ (or "ICO"). For the two cases $\hat{a}_0 = -1, 0$ (corresponding to their $\kappa_i = -1, 0$), they found, in the 3PN-NLO case, energy minima equal to $e \equiv E_{\rm ICO}/m = -0.0116, -0.0193$ for corresponding orbital frequencies $\hat{\Omega} \equiv m\omega_{\rm ICO} = 0.059, 0.129$. These numerical values should be compared with the numerical values we quote in Table I below. On the other hand, for the large and parallel spin case $\hat{a}_0 = +1$ Ref. [15] found that the Taylor-expanded function $e^{\rm Taylor}(\hat{\Omega})$ has no minimum. Finally, note that the qualitative shape of the curve giving the (EOB) LSO energy as a function of the spin parameters $\hat{a}_0$ is similar both to the corresponding

[18] As we recalled above, spinning binaries admit, in general, only *spherical* orbits, rather than *circular* ones. Reference [1] studied the binding energies of the Last Stable Spherical Orbits (LSSO). Here, however, we restrict ourselves to the parallel spin, where it makes sense to study circular, equatorial orbits.

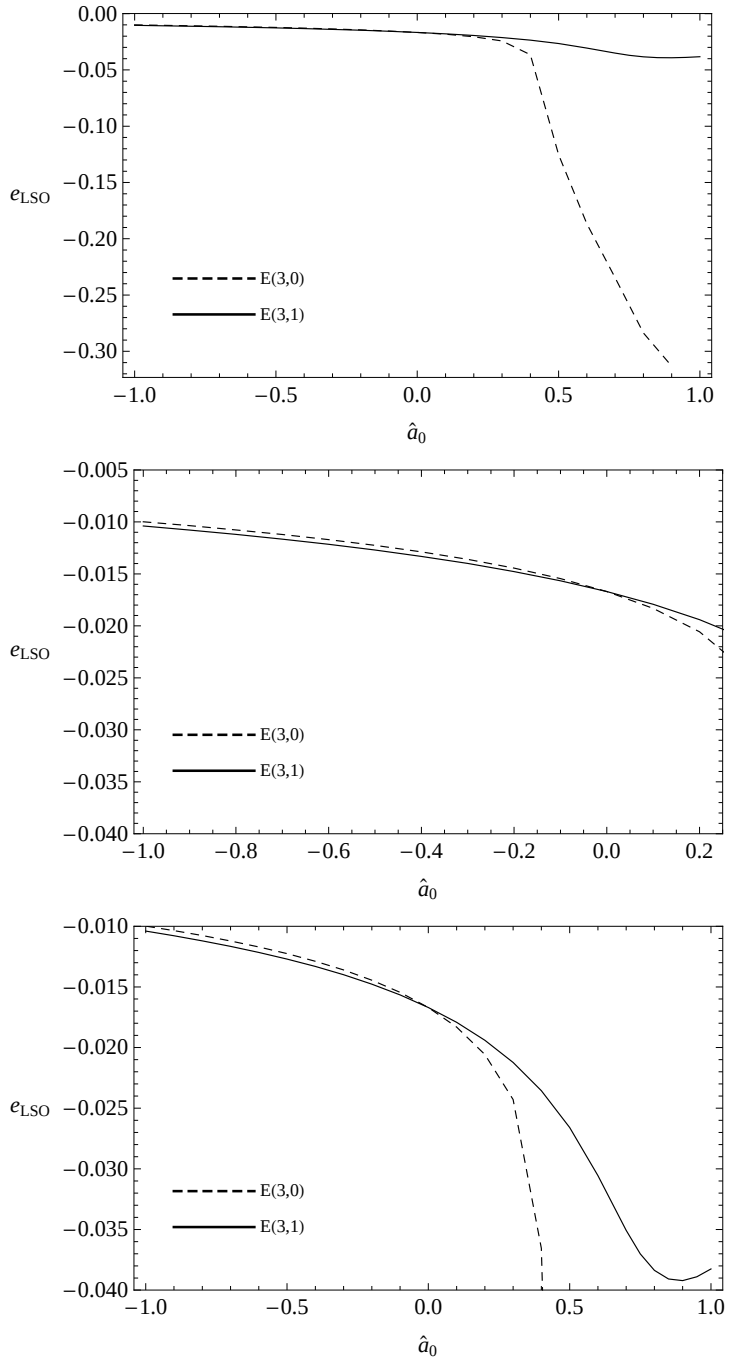

FIG. 4: Binding energy of the Last Stable (circular) Orbit (LSO) predicted by the EOB approach. We study the effect of including NLO spin-orbit terms by contrasting the LO and NLO predictions. We plot the dimensionless energy $e_{\rm LSO}$ of the LSO versus $\hat{a}_0$. We have assumed $m_1 = m_2$, $a_1 = a_2$, and $\theta_0 = \pi/2$. For E$(3,0)$ a LSO exists up to $\hat{a}_0 \leq +0.9$.

curve for a spinless test-particle in a Kerr background (see, e.g., Fig. 7 below), and to the curve giving the LSO energy of a *spinning test particle* in a Kerr background, as a function of the test spin (see Fig. 4 in Ref. [24]).

To complement the information displayed in Figs. 1–4, we give in Table I the numerical values of the main LSO characteristics (binding energy and orbital frequency) for our "best bet" Hamiltonian, namely the 3PN-NLO EOB one E$(3,1)$.

In Figs. 5 and 6 we study the effective-spin-dependence of another LSO-related physical quantity of relevance for the dynamics of coalescing binaries: the total (orbital plus spin) angular momentum of the binary when it reaches

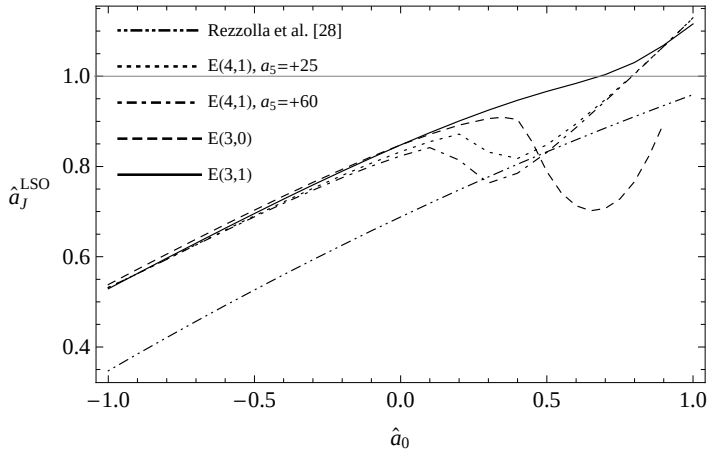

FIG. 5: The dimensionless total angular momentum Kerr parameter $\hat{a}_J^{\rm LSO}$, Eq. (5.13), at the LSO, versus $\hat{a}_0$. We have assumed $m_1 = m_2$, $a_1 = a_2$, and $\theta_0 = \pi/2$. The parameter $\hat{a}_J^{\rm LSO}$ is computed from Eq. (5.13) with $\hat{j}_{\rm LSO} = \hat{\ell}_{\rm LSO} + \hat{a}_1 + \hat{a}_2 = \hat{\ell}_{\rm LSO} + 2\hat{a}_0$. We compare the various EOB predictions obtained either by improving the accuracy of spin-orbit terms [E(3, 1) versus E(3, 0)], or by improving the accuracy of orbital terms [E(4, 1) versus E(3, 1)]. We use two representative values of the 4PN parameter $a_5 = +25$ and $a_5 = +60$. For comparison, we also include a fit to recent numerical estimates of the *final* Kerr parameter of the black hole resulting from the coalescence of the two constituent black holes.

the LSO [i.e., at the end of the (approximately) adiabatic inspiral, just before the plunge],

$$\mathbf{J} \equiv \mathbf{L} + \mathbf{S}_1 + \mathbf{S}_2. \tag{5.11}$$

In terms of rescaled dimensionless variables, this becomes

$$\hat{\mathbf{j}} \equiv \frac{c}{GM\mu}\mathbf{J} = \hat{\boldsymbol{\ell}} + \frac{m_1}{m_2}\hat{\mathbf{a}}_1 + \frac{m_2}{m_1}\hat{\mathbf{a}}_2, \tag{5.12}$$

where $\hat{\boldsymbol{\ell}} \equiv c\,\boldsymbol{\ell}$. Actually, the most relevant quantity is the dimensionless Kerr parameter associated to the total LSO mass-energy and the total LSO angular momentum, i.e., the value at the LSO of the ratio

$$\hat{a}_J \equiv \frac{cJ}{G\big(H_{\rm real}/c^2\big)^2} = \nu \frac{\hat{j}}{\big(H_{\rm real}/(Mc^2)\big)^2}, \tag{5.13}$$

where $\hat{j}$ is the modulus of $\hat{\mathbf{j}}$.

- In Fig. 5 we contrast the dependence of $\hat{a}_J^{\rm LSO}$ on the dimensionless effective spin parameter $\hat{a}_0$ for several EOB models: the two 3PN-accurate ones [E(3, 0) using LO-accurate spin-orbit, and E(3, 1) using NLO-accurate spin-orbit], and two illustrative [7, 9] "4PN-accurate" NLO-spin-orbit models E(4, 1) (using either $a_5 = +25$ or $a_5 = +60$, as in Fig. 1). [Here, we are still considering fully symmetric systems with $m_1 = m_2$ and $a_1 = a_2$, so that $\hat{a}_0 = \hat{a}_1 = \hat{a}_2$.] Again we see the moderating influence of NLO corrections. The EOB-LO curve E(3, 0) exhibits a sudden drop down (pointed out in [1]) before rising up again (and disappearing at $\hat{a}_0 = +0.9$ when the LSO ceases to exist). By contrast, the NLO curve E(3, 1) exhibits a much more regular dependence on $\hat{a}_0$, which is roughly linear over the entire range of values $-1 \leq \hat{a}_0 \leq 1$. The two illustrative E(4, 1) curves exhibit a "mixed" behaviour where a "drop" similar to the one featuring in the LO curve is still present, though it is moderated by NLO spin-orbit effects. This sensitivity to the inclusion of a 4PN contribution in $A(\hat{u})$ is due to a delicate interplay between the modified shape of the basic spin-independent "radial potential" $A(\hat{u}, a_5)$ and the use of a (1,4) Padé resummation of the "effective spin-dependent radial potential" $\Delta_t(R)$, Eq. (4.6a). Indeed, the additional contributions proportional to a_5 and a^2 are *both repulsive* , and tend to compound their effect, which is to push the LSO toward closer, more bound orbits [1].

  We have also indicated in Fig. 5 the *final* (i.e., after coalescence) dimensionless Kerr parameter of (symmetric) spinning binaries, as obtained in recent numerical simulations [26, 27, 28, 29]. For simplicity, we have shown the simple analytic fit proposed in [28]. The fact that the 3PN-NLO-accurate EOB LSO Kerr parameter [E(3, 1)] is systematically *above* the final Kerr parameter is in good agreement with the fact that, after reaching the

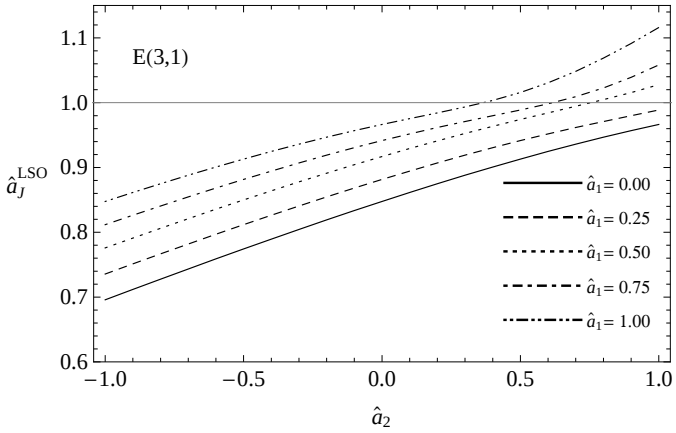

FIG. 6: The dimensionless total angular momentum Kerr parameter $\hat{a}_J^{\rm LSO}$ at the E(3,1) LSO versus $\hat{a}_2$ for various values of the parameter $\hat{a}_1$. Here we consider spin-dissymmetric systems with $a_1 \neq a_2$ (but still $m_1 = m_2$ and $\theta_0 = \pi/2$). The parameter $\hat{a}_J^{\rm LSO}$ is computed from Eq. (5.13) with $\hat{j}_{\rm LSO} = \hat{\ell}_{\rm LSO} + \hat{a}_1 + \hat{a}_2$.

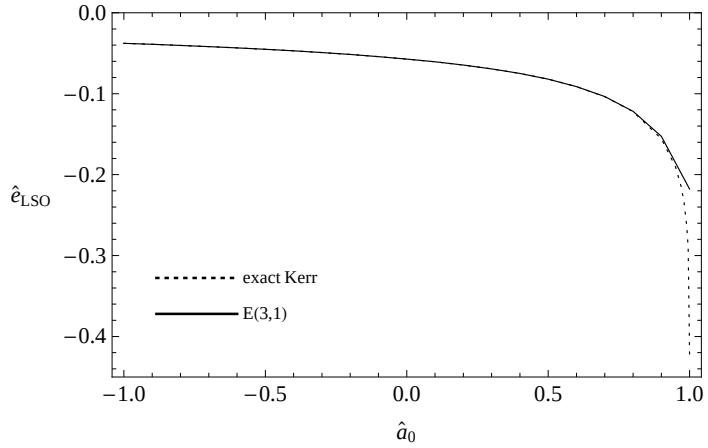

FIG. 7: Comparison of the test-mass limit $m_2 \simeq \mu \to 0$ (with fixed $\hat{a}_2$; so that $S_2/m_2 \to 0$) for two Hamiltonians. We consider the specific "non relativistic" binding energy $\hat{e}_{\rm LSO} \equiv e_{\rm LSO}/\nu = (E_{\rm LSO} - Mc^2)/(\mu c^2)$ at the LSO versus $\hat{a}_0$. The solid curve is the result of taking the test-mass limit of the EOB Hamiltonian, while the short-dashed curve is the result for a test particle moving in the Kerr spacetime.

LSO, the system will still loose a significant amount of angular momentum[19] during the plunge and the merger-plus-ringdown. In the case of *non-spinning* binaries, it has been shown that, by using the EOB formalism up to the end of the process [i.e., by taking into account the losses of J and E during plunge, as well as during merger-plus-ringdown], there was a good agreement (better than $\sim 2\%$) between EOB and numerical relativity for the final spin parameter [12]. We hope that the same type of agreement will hold also in the case of *spinning* binaries considered here.

- In Fig. 6 we plot the LSO dimensionless Kerr parameter of Eq. (5.13) for *spin-dissymmetric* systems, namely $a_1 \neq a_2$ (but with $m_1 = m_2$), computed with the 3PN-NLO EOB Hamiltonian model E(3, 1). This plot illustrates that the LSO spin parameter is a smooth (and essentially linear) function of the two individual spins.

- Finally, we compare in Fig. 7 the spinless test particle limit [i.e., $m_2 \to 0$, together with $a_2 = S_2/(m_2 c) \to 0$, as appropriate to black holes for which $\hat{a} \leq 1$] for two Hamiltonians: the 3PN-NLO EOB one E(3, 1), and the exact

[19] We use here the fact (found in numerical calculations, and implied by the analytical EOB approach), that, fractionally speaking, the angular momentum loss after the LSO is significantly higher than the corresponding energy loss.

one, as known from the geodesic action of a spinless test particle in the Kerr metric. For non-spinning systems the EOB Hamiltonian is constructed so as to reduce to the exact Schwarzschild-derived one in the test-particle limit. However, for spinning systems, we have chosen in Eq. (4.6a) to define the crucial metric coefficient $\Delta_t(R)$ by Padé-resumming the sum of $A(R;\nu)+a^2/R^2$. This Padé-resummation is indeed useful for generally ensuring, for comparable mass systems, that $\Delta_t(R)$ have a simple zero at some "effective horizon" $r_{\rm H}$. However, in the test-mass limit $\nu \to 0$, while the Taylor-approximant to $A(R;\nu) + a^2/R^2$ would coincide with the exact Kerr answer, the Padé-resummed version of $A(R;\nu) + a^2/R^2$ differs from it. We see, however, on Fig. 7 that the resulting difference has a very small effect on the LSO energy per unit (μ) mass, except when the dimensionless effective spin $\hat{a}_0$ is very close to $+1$. On the other hand, as we saw above when discussing Fig. 5, the issue of the Padé resummation of $\Delta_t(R)$ becomes more subtle when one considers the comparable-mass case, together with the inclusion of a repulsive 4PN parameter a_5.

VI. CONCLUSIONS

The main conclusions of this work are:

- We have prepared the ground for an accurate Effective One Body (EOB) description of the dynamics of binary systems made of *spinning* black holes by incorporating the recent computation of the next-to-leading order (NLO) spin-orbit interaction Hamiltonian [13] (see also Refs. [14, 15]) into a previously developed extension of the EOB approach to spinning bodies [1].

- We found that the inclusion of NLO spin-coupling terms has the quite significant result of *moderating* the effect of the LO spin-coupling, which would, by itself (as found in Ref. [1]), predict that the Last Stable (circular) Orbit (LSO) of parallely-fast-spinning black holes can reach very large binding energies of the order of 30% of the total rest-mass energy Mc^2. By contrast, the inclusion of NLO spin-orbit terms predicts that the LSO of parallely-fast-spinning systems, though significantly more bound than that of non-spinning holes, can only reach binding energies of the order of 4% of the total rest-mass energy Mc^2 (see Fig. 4 above). This reduction in the influence of the spin-orbit coupling is due to the fact that the (effective) "gyro-gravitomagnetic ratios" are *reduced* by NLO effects from their LO values $g_S^{\rm LO}=2$, $g_{S^*}^{\rm LO}=\frac{3}{2}$ to the values (here considered along circular orbits)

$$\begin{aligned} g_S^{\rm circ\,eff} &= 2 - \frac{5}{8}\nu x, \\ g_{S^*}^{\rm circ\,eff} &= \frac{3}{2} - \Big(\frac{9}{8}+\frac{3}{4}\nu\Big)x, \end{aligned} \tag{6.1}$$

  where $x \simeq GM/(Rc^2) \simeq (GM\Omega/c^3)^{2/3}$. This reduction then reduces the *repulsive* effect of the spin-orbit coupling which is responsible for allowing the binary system to orbit on very close, and very bound, orbits (see discussion in Section 3C of Ref. [1]).

- We studied the dependence of the dimensionless Kerr parameter of the binary system, $\hat{a}_J \equiv cJ/\big(G(H_{\rm real}/c^2)^2\big)$, computed at the LSO, on the spins of the constituent black holes. Again the moderating effect of including NLO spin-orbit terms is very significant (compare the solid and the dashed[20] lines in Fig. 5). Thanks to this moderating effect the LSO Kerr parameter $\hat{a}_J^{\rm LSO}$ is found to have a monotonic, and roughly linear, dependence on the spin parameters of the individual black holes (see solid line in Fig. 5 and the various curves in Fig. 6). We also studied the effect of including the type of 4PN parameter a_5 found useful in recent work [7, 8, 9, 10] for improving the agreement between EOB waveforms and numerical ones.

- We leave to future work the analog of what was initiated for spinning systems in Ref. [5], and recently completed for the case of non-spinning black holes in Ref. [12], i.e., a full dynamical study, within the EOB approach, of the Kerr parameter of the *final* black hole resulting from the merger of spinning black holes which takes into account the angular momentum losses that occur after the LSO, during the plunge, the merger, and the ringdown. Let us also note that Ref. [30] has recently proposed an approximate analytical approach (which is similar in spirit

[20] Compare also with Fig. 2 of Ref. [1] where the relevant LO result is the curve labelled "DJS" which reaches a maximum around $\hat{a} \equiv \frac{7}{8}\hat{a}_0 \simeq 0.31$, in agreement with the (local) maximum in the dashed line of our Fig. 5 reached around $\hat{a}_0 \simeq 0.36$.

to the approximation used in Refs. [1, 3, 5] and above, namely that of considering the Kerr parameter of an effective test particle at, or after, the LSO) towards estimating the final spin of a binary black hole coalescence. The resulting prediction is, however, only in coarse agreement $\sim 10\%$ with numerical results. Note in this respect that, as displayed in Fig. 5, the "zeroth order" EOB result [corresponding to using the Kerr parameter for E(3, 1) at the LSO, without taking into account the later losses of angular momentum] is already in $\sim 20\%$ agreement with the fit to the numerical data [28]. The fact (displayed on Fig. 5) that the E(3,1) EOB LSO Kerr parameter is systematically *above* the final (after coalescence) Kerr parameter determined by recent numerical simulations [26, 27, 28, 29] is in qualitative agreement with the fact that the system will loose a significant amount of angular momentum during the plunge and the merger-plus-ringdown. Note, however, the sensitivity of $\hat{a}_J^{\rm LSO}$ to a "4PN deformation" of the EOB Hamiltonian by the parameter a_5. As said above, this sensitivity is due to the fact that the radial function $\Delta_t(R)/R^2$ combines the additional repulsive effects of both a positive 4PN contribution $+a_5\nu\big(GM/(c^2R)\big)^5$ and a positive spin-dependent contribution $+a^2/R^2$. We leave to future work an exploration of this issue, which might need the use of a different Padé resummation than the (1,4) one used in (4.6a).

It remains to be seen whether the EOB/Numerical Relativity comparison for the final Kerr parameter of spinning systems will be as good as it was found to be for the non-spinning case [12], i.e., at the 2% level. If this is the case, it will establish the physical relevance of the improved EOB Hamiltonian constructed in the present paper.

- Let us finally note that there is some *flexibility* in the improved spin-dependent EOB Hamiltonian proposed above (besides the flexibility in the choice of the Padé resummation mentioned above). On the one hand, the choice (3.14) for the gauge parameters $a(\nu)$ and $b(\nu)$ might be replaced by other choices. On the other hand, the choice (4.11) for the effective spin vector might also be replaced by other ones. In particular, it might be interesting to consider the alternative definition

$$\begin{aligned} Mc\,\mathbf{a}_{\rm new} \equiv \mathbf{S}_{\rm eff\,new} &\equiv \frac{1}{2} g_S^{\rm eff\,new} \mathbf{S}_0 \\ &= \frac{1}{2} g_S^{\rm eff\,new} \big(\mathbf{S} + \mathbf{S}^*\big). \end{aligned} \tag{6.2}$$

This definition coincides with the one used above at LO in spin-orbit effects (because $g_S^{\rm eff\,new} = 2 + \mathcal{O}(\nu/c^2)$), and allows one to use a simplified supplementary spin-orbit contribution, built with

$$\boldsymbol{\sigma}^{\rm new} \equiv \frac{1}{2}\big(g_{S^*}^{\rm eff} - g_S^{\rm eff}\big)\mathbf{S}^*, \tag{6.3}$$

instead of (4.15). It might be interesting to explore which of these possible definitions exhibits the best agreement with current numerical results.

Acknowledgments

This work was supported in part by the KBN Grant no 1 P03B 029 27 (to P.J.) and by the Deutsche Forschungsgemeinschaft (DFG) through SFB/TR7 "Gravitational Wave Astronomy".

[1] T. Damour, "Coalescence of two spinning black holes: An effective one-body approach," Phys. Rev. D **64**, 124013 (2001) [arXiv:gr-qc/0103018].

[2] A. Buonanno and T. Damour, "Effective one-body approach to general relativistic two-body dynamics," Phys. Rev. D **59**, 084006 (1999) [arXiv:gr-qc/9811091].

[3] A. Buonanno and T. Damour, "Transition from inspiral to plunge in binary black hole coalescences," Phys. Rev. D **62**, 064015 (2000) [arXiv:gr-qc/0001013].

[4] T. Damour, P. Jaranowski, and G. Schäfer, "On the determination of the last stable orbit for circular general relativistic binaries at the third post-Newtonian approximation," Phys. Rev. D **62**, 084011 (2000) [arXiv:gr-qc/0005034].

[5] A. Buonanno, Y. Chen, and T. Damour, "Transition from inspiral to plunge in precessing binaries of spinning black holes," Phys. Rev. D **74**, 104005 (2006) [arXiv:gr-qc/0508067].

[6] T. Damour and A. Nagar, "Faithful Effective-One-Body waveforms of small-mass-ratio coalescing black-hole binaries," Phys. Rev. D **76**, 064028 (2007) [arXiv:0705.2519 [gr-qc]].

[7] A. Buonanno, Y. Pan, J. G. Baker, J. Centrella, B. J. Kelly, S. T. McWilliams, and J. R. van Meter, "Toward faithful templates for non-spinning binary black holes using the effective-one-body approach," Phys. Rev. D **76**, 104049 (2007) [arXiv:0706.3732 [gr-qc]].

[8] T. Damour and A. Nagar, "Comparing Effective-One-Body gravitational waveforms to accurate numerical data," Phys. Rev. D **77**, 024043 (2008) [arXiv:0711.2628 [gr-qc]].

[9] T. Damour, A. Nagar, E. N. Dorband, D. Pollney, and L. Rezzolla, "Faithful Effective-One-Body waveforms of equal-mass coalescing black-hole binaries," arXiv:0712.3003 [gr-qc].

[10] T. Damour, A. Nagar et al., in preparation.

[11] F. Pretorius, "Binary black hole coalescence," arXiv:0710.1338 [gr-qc].

[12] T. Damour and A. Nagar, "Final spin of a coalescing black-hole binary: An effective-one-body approach," Phys. Rev. D **76**, 044003 (2007) [arXiv:0704.3550 [gr-qc]].

[13] T. Damour, P. Jaranowski, and G. Schäfer, "Hamiltonian of two spinning compact bodies with next-to-leading order gravitational spin-orbit coupling," arXiv:0711.1048 [gr-qc].

[14] G. Faye, L. Blanchet, and A. Buonanno, "Higher-order spin effects in the dynamics of compact binaries. I: Equations of motion," Phys. Rev. D **74**, 104033 (2006) [arXiv:gr-qc/0605139].

[15] L. Blanchet, A. Buonanno, and G. Faye, "Higher-order spin effects in the dynamics of compact binaries. II: Radiation field," Phys. Rev. D **74**, 104034 (2006) [Erratum-ibid. D **75**, 049903 (2007)] [arXiv:gr-qc/0605140].

[16] B. M. Barker and R. F. O'Connell, "Derivation of the equations of motion of a gyroscope from the quantum theory of gravitation," Phys. Rev. D **2**, 1428 (1970).

[17] J. Steinhoff, S. Hergt, and G. Schäfer, "On the next-to-leading order gravitational spin(1)-spin(2) dynamics," arXiv:0712.1716 [gr-qc].

[18] T. Damour, P. Jaranowski, and G. Schäfer, "Poincaré invariance in the ADM Hamiltonian approach to the general relativistic two-body problem," Phys. Rev. D **62**, 021501 (2000) [Erratum-ibid. D **63**, 029903 (2001)] [arXiv:gr-qc/0003051].

[19] T. Damour, P. Jaranowski, and G. Schäfer, "Dimensional regularization of the gravitational interaction of point masses," Phys. Lett. B **513**, 147 (2001) [arXiv:gr-qc/0105038].

[20] T. Damour, M. Soffel, and C. Xu, "General relativistic celestial mechanics. 1. Method and definition of reference systems," Phys. Rev. D **43**, 3273 (1991).

[21] T. Damour, M. Soffel, and C. Xu, "General relativistic celestial mechanics. 3. Rotational equations of motion," Phys. Rev. D **47**, 3124 (1993).

[22] T. Damour and J. H. Taylor, "Strong field tests of relativistic gravity and binary pulsars," Phys. Rev. D **45**, 1840 (1992).

[23] L. Blanchet, "Innermost circular orbit of binary black holes at the third post-Newtonian approximation," Phys. Rev. D **65**, 124009 (2002) [arXiv:gr-qc/0112056].

[24] S. Suzuki and K. Maeda, "Innermost stable circular orbit of a spinning particle in Kerr spacetime," Phys. Rev. D **58**, 023005 (1998) [arXiv:gr-qc/9712095].

[25] M. Campanelli, C. O. Lousto, Y. Zlochower, B. Krishnan, and D. Merritt, "Spin flips and precession in black-hole-binary mergers," Phys. Rev. D **75**, 064030 (2007) [arXiv:gr-qc/0612076].

[26] F. Herrmann, I. Hinder, D. M. Shoemaker, P. Laguna, and R. A. Matzner, "Binary black holes: Spin dynamics and gravitational recoil," Phys. Rev. D **76**, 084032 (2007) [arXiv:0706.2541 [gr-qc]].

[27] P. Marronetti, W. Tichy, B. Brugmann, J. Gonzalez, and U. Sperhake, "High-spin binary black hole mergers," arXiv:0709.2160 [gr-qc].

[28] L. Rezzolla, E. N. Dorband, C. Reisswig, P. Diener, D. Pollney, E. Schnetter, and B. Szilagyi, "Spin diagrams for equal-mass black-hole binaries with aligned spins," arXiv:0708.3999 [gr-qc].

[29] L. Rezzolla, P. Diener, E. N. Dorband, D. Pollney, C. Reisswig, E. Schnetter, and J. Seiler, "The final spin from the coalescence of aligned-spin black-hole binaries," arXiv:0710.3345 [gr-qc].

[30] A. Buonanno, L. E. Kidder, and L. Lehner, "Estimating the final spin of a binary black hole coalescence," Phys. Rev. D **77**, 026004 (2008) [arXiv:0709.3839 [astro-ph]].